STUDY ON THE BEHAVIOR OF LIGHT ON EROSION IN EPOXY COATING ON SS316L

Dissertation submitted in partial fulfilment of the requirements

for the award of degree

of

Master of Technology in Marine Technology

by

NATTATH SREEJITH DAS

(Regd. No: 2301215003)

Under the Supervision of

Dr. NACHIKETA DAS

&

Dr. ADITYA KOLAKOTI

Department of Marine Engineering

Indian Maritime University, Kolkata Campus

Kolkata - 700088

June 2025

INDIAN MARITIME UNIVERSITY KOLKATA CAMPUS

Department of Marine Engineering

CERTIFICATE

This is to certify that the thesis entitled **" STUDY ON THE BEHAVIOR OF LIGHT ON EROSION IN EPOXY COATING ON SS316L " submitted by Mr. NATTATH SREEJITH DAS (2301215003) of the Department of Marine Engineering, Indian Maritime University (Kolkata Campus),** in partial fulfilment of the requirements for the award of the degree of Master of Technology in Marine Technology, is a record of Bonafide research work carried out under my supervision and guidance. The content of the dissertation does not form a basis for the award of other degrees to his/her, to the best of my knowledge. The dissertation, in my opinion, is worthy of consideration for the award of the degree of Master of Technology in Marine Technology in accordance with the regulation of the Institute.

Dr. Nachiketa Das
Supervisor
Indian Maritime University,
Kolkata Campus
Kolkata, West Bengal
700088 India

Dr. Aditya Kolakoti
Course Co-ordinator
& Co-Supervisor
Indian Maritime University,
Kolkata Campus
Kolkata,
West Bengal
700088
India

Mr. Hare Ram Hare
External Examiner
Assistant Professor
Indian Maritime
University,
Mumbai Port Campus,
Mumbai,
Maharashtra
400033 India

EVALUATION SHEET

Name of Candidate	NATTATH SREEJITH DAS
Title of the project	STUDY ON THE BEHAVIOR OF LIGHT ON EROSION IN EPOXY COATING ON SS316L.
Specialization	Marine Technology
Date of Examination	27/05/2025

The board approved this dissertation for the exam

External Examiner:

Internal Examiner:

COPYRIGHT AND CONSENT FORM

To ensure uniformity of treatment among all contributors, other forms may not be substituted for this form, nor may any wording of the form be changed. This form is intended for original material submitted to the Indian Maritime University, Kolkata Campus (IMU-KC), Kolkata and must accompany any such material in order to be published by the (IMU-KC) Please read the form carefully and keep a copy for your files.

TITLE OF THESIS: STUDY ON THE BEHAVIOR OF LIGHT ON EROSION IN EPOXY COATING ON SS316L.

AUTHOR'S NAME and ADDRESS: 29-7/1.PADMASAROVARAM HOUSE, SVLND LAYOUT PHASE 2, VEPAGUNTA, VISAKHAPTNAM-530047. ANDHRA PRADESH. INDIA.

COPY RIGHT TRANSFER

The undersigned hereby assigns to Indian Maritime University, Kolkata Campus (IMU-KC), Kolkata, all rights under copyright that may exist in and to: (a) the above work, including any revised or expanded derivative works submitted to the (IMU-KC), by the undersigned based on the work and (b) any associated written or multimedia components or other enhancements accompanying the work.

CONSENT AND RELEASE

In the event the undersigned makes a presentation based upon the work at a conference hosted or sponsored in whole or in part by the (IMU-KC), the undersigned, in consideration for his/her participation in the conference, hereby grants the (IMU-KC), the unlimited, worldwide, irrevocable permission to use, distribute, publish, license, exhibit, record, digitize, broadcast, reproduce and archive; in any format or medium, whether now known or hereafter developed:

a) His/her presentation and comments at the conference;

b) Any written materials or multimedia files used in connection with his/her presentation and

c) Any recorded interview him/her (collectively, the "Presentation").

The permission granted includes the transcription and reproduction of the Presentation for inclusion in products sold or distributed by (IMU-KC) and live or recorded broadcast of the Presentation during or after the conference.

In connection with the permission granted in Section 2, the undersigned hereby grants (IMUKC) the unlimited, worldwide, irrevocable right to use his/her name, picture, likeness, voice and biographical information as part of the advertisement, distribution and sale of products incorporating the Work or Presentation, and releases (IMU-KC) from any claim based on right of privacy or publicity.

The undersigned hereby warrants that the Work and Presentation (collectively, the "Materials") are original and that he/she is the author of the Materials. To the extent the Materials incorporate test passages, figures, data or other material from the works of others, the undersigned has obtained any necessary permissions.

GENERAL TERMS

- The undersigned represents that he/she has the power and authority to make and execute this assignment.

- The undersigned agrees to indemnify and hold harmless the (IMU-KC) from any damage or expense that may arise in the event of a breach of any of the warranties set forth above.

- In the event the above work is not accepted and published by the (IMU-KC) or is withdrawn by the author(s) before acceptance be the (IMU-KC), the foregoing copyright transfer shall become null and void and all materials embodying the work submitted to the (IMU-KC) will be destroyed.

- For jointly authored works, all joint authors should sign, or one of the authors should sign as authorized agent for the others.

NATTATH SREEJITH DAS
(Regd. No: 2301215003)

TABLE OF CONTENT

Page No.

ACKNOWLEDGEMENT

I want to take this opportunity to express sincere thanks and appreciation to everyone who helped me finish my project and create this project report. I extend my heartfelt thanks to RAdm. AMIT BOSE (Retd), our esteemed Director of IMU Kolkata Campus, for his unwavering support, encouragement, and provision of library and laboratory facilities for the Preparation of this report.

I seize this opportunity to convey our deepest gratitude and utmost respect to my supervisor and mentor, Dr. NACHIKETA DAS & Dr. ADITYA KOLAKOTI, from the Department of Marine Engineering, for his exceptional guidance, diligent supervision, and constant motivation throughout the project's duration. His invaluable support, immense assistance, wholehearted cooperation, and fruitful discussions throughout the semester are encapsulated within this dissertation.

I want to thank Dr. ADITYA KOLAKOTI, our course coordinator, Department of Marine Engineering, IMU Kolkata, for his guidance, assistance, encouragement, and support in getting this project done. His organizational skills and prompt assistance helped us overcome various challenges and ensured the smooth progression of my work.

Additionally, I would like to thank the Indian Maritime University Kolkata for their support and cooperation in making this research possible by providing the facilities and resources needed. The help they provided was crucial to the accomplishment of the project.

Lastly, I extend my thanks to all those who were involved, directly or indirectly, during the course of this project.

DECLARATION

I certify that

a) The work contained in this thesis is original and has been done by me under the guidance of my supervisor.

b) The work has not been submitted to any other Institute for any degree.

c) I have followed the guidelines provided by the Institute in preparing the thesis.

d) I have conformed to the norms and guidelines given in the Ethical Code of Conduct of the Institute.

e) Whenever I have used materials (data, theoretical analysis, figures, and text) from other sources, I have given due credit to them by citing them in the text of the thesis and giving their details in the references.

NATTATH SREEJITH DAS.
(Regd no: 2301215003)

LIST OF FIGURES

Page No.

Figure 08

- Erosion vs Deviation plot for (vi), (vii), (viii)- (Pure Epoxy, Epoxy + 0.1% Graphene, Epoxy + 1% Graphene)

Figure 09

- Capacitance vs Deviation (RG,BG,RB) plot for (x), (xi), (xii)- (Pure Epoxy, Epoxy + 0.1% Graphene.

LIST OF TABLES

Page No.

LIST OF ABBREVIATION

Abbreviation	Full Form
SS316L	Austenitic Stainless Steel 316L
SiC	Silicon Carbide
wt.%	Weight Percent
ASTM	American Society for Testing and Materials
Ra	Average Surface Roughness
RGB	Red-Green-Blue (Color Model)
RG	Red-Green Filter Combination
BG	Blue-Green Filter Combination
RB	Red-Blue Filter Combination
Ep	Energy Index
SCY	Structural Color Aliasing Index
MAE	Mean Absolute Error
PLCC	Pearson Linear Correlation Coefficient
nm	Nanometer
µm	Micrometer
EIS	Electrochemical Impedance Spectroscopy
SEM	Scanning Electron Microscopy
FFT	Fast Fourier Transform
CDSM	Color Distribution Statistical Matrix
HVS	Human Visual System

MWCNTs	Multi-Walled Carbon Nanotubes
NDE	Non-Destructive Evaluation
GLCM	Gray-Level Co-occurrence Matrix
CNC	Computer Numerical Control
NIR	Near Infrared
dpi	Dots Per Inch
Tmax	Maximum Thickness (used in erosion calculations)
T	Measured Thickness (used in erosion calculations)
Epoxy + GNP	Epoxy with Graphene Nanoplatelets
RGB M	Mean value of RGB channels
R, G, B	Red, Green, Blue (color channels)
CD	Color Difference
F	Sharpness Index

ABSTRACT

This research employs optical analysis, and light intensity analysis with, three coating systems—pure epoxy, epoxy with 0.1 wt.% graphene, and epoxy with 1 wt.% graphene—were systematically evaluated for their erosion resistance and optical characteristics on SS316L stainless steel substrates. The coating thicknesses ranged from 85 µm to 103 µm, with erosion factor calculated as the reduction from the maximum thickness (103 µm). Pure epoxy exhibited the highest erosion factor of 18 µm, followed by 11 µm for epoxy + 0.1% graphene, and as low as 5 µm for epoxy + 1% graphene, indicating improved erosion resistance with increasing graphene content. Surface roughness (Ra) measurements showed a corresponding rise due to erosion, increasing from approximately 0.33 µm to 1.12 µm for pure epoxy, whereas the increase was limited from 0.19 µm to 0.45 µm in epoxy + 1% graphene coatings, highlighting the protective advantage of graphene modification. Optical analysis using RGB light filters further revealed a progressive increase in deviation values with erosion severity, where pure epoxy exhibited a maximum deviation of 0.165 at highest erosion, compared to only 0.025 for epoxy + 0.1% graphene and 0.008 for epoxy + 1% graphene at lower erosion levels. Additionally, the Energy Index (Ep), sensitive to nanoscale surface roughness, demonstrated a strong inverse correlation with Ra (Pearson Linear Correlation Coefficient, PLCC = 0.91; Mean Absolute Error, MAE = 10.7 nm), while the Structural Color Aliasing Index (SCY) effectively captured macro-level degradation, showing higher correlation (PLCC = 0.93) and a MAE of 0.12 µm. These findings not only confirm the erosion mitigation capability of graphene-reinforced coatings but also establish a robust foundation for non-destructive, real-time optical monitoring of coating health using structured light and digital image-based metrics.

CHAPTER 1

INTRODUCTION

1.1 Significance

The relentless degradation of materials due to erosion poses a significant challenge across various engineering domains, impacting the lifespan and performance of critical components in industries ranging from aerospace to marine engineering. The previous Study focused primarily on mechanical and electrical aspects of erosion in epoxy coatings, neglecting optical degradation. The lack of optical characterization limits the ability to detect early-stage erosion and predict coating lifespan. The behavior of pure epoxy and epoxy-graphene composite coatings applied to 316L stainless steel substrates. 316L stainless steel, widely used in marine, biomedical, automotive, and structural applications, is prone to corrosion in aggressive environments such as seawater. Protective coatings such as epoxy are applied to improve corrosion resistance and extend the service life of metal structures.

However, the long-term stability of these coatings depends on both mechanical and electrical properties, especially under erosion. In recent years, the integration of nanomaterials like graphene into epoxy resins has emerged as a promising approach to enhance coating performance by improving barrier properties, mechanical strength, and electrical stability. Further, Incorporation of graphene into epoxy coatings significantly enhances mechanical and electrical properties. Epoxy + 0.1 wt.% graphene composite provided optimal balance between mechanical integrity, surface roughness, and electrical insulation. The erosion-induced degradation was minimized with graphene-modified coatings, offering superior long-term stability. The novel approach of optical characterization through light intensity and deviation provided additional insight into coating degradation and opened possibilities for non-contact inspection techniques. Among the various forms of material degradation, erosion-corrosion, a synergistic process involving the combined effects of mechanical wear and electrochemical corrosion, presents a particularly insidious threat (Kucharczyk et al., 2021) [1]. This phenomenon is especially prominent in flow systems, where the impingement of abrasive particles or high-velocity fluids accelerates the corrosion rate of metallic structures (Cheng, 2011) [2]. To combat the detrimental effects of erosion-corrosion, protective coatings are

frequently employed as a barrier between the metallic substrate and the corrosive environment (Policastro et al., 2011) [3]. Epoxy coatings, renowned for their excellent adhesion, chemical resistance, and ease of application, have emerged as a popular choice for safeguarding metallic surfaces against corrosion (Li et al., 2021) [4]. Despite their widespread use, epoxy coatings are not immune to erosion damage, and their long-term performance hinges on their ability to withstand the combined effects of mechanical wear and chemical attack. Understanding the optical characteristics of erosion in epoxy coatings is crucial for developing effective strategies to mitigate material degradation and enhance the durability of coated structures (Ayodeji et al., 2021) [5]. Epoxy coatings offer a cost-effective approach to shield steel from corrosion, showcasing the potential to create robust, durable, and corrosion-resistant layers (SWAMY & Koyama, 1989) [6].

The utilization of epoxy coatings on SS316L stainless steel is prevalent in various industrial applications, primarily due to the coatings' ability to provide a barrier against corrosive environments and mechanical wear (Łyczkowska-Widłak et al., 2018) [7]. Epoxy resins, known for their excellent adhesion, chemical resistance, and mechanical strength, serve as a protective layer, extending the lifespan and maintaining the structural integrity of the underlying SS316L substrate (Stango et al., 2017) [8]. However, these coatings are inevitably subjected to erosive forces, whether from solid particle impingement, liquid droplet impact, or cavitation, leading to gradual material removal and eventual substrate exposure (Sanjuán & Toro, 2010) [9]. The erosion process not only compromises the protective function of the coating but also alters its surface characteristics, which can be observed and quantified through optical means.

Understanding the optical characteristics of erosion in epoxy coatings is crucial for developing non-destructive evaluation techniques and predicting the remaining service life of coated components. Optical techniques offer a non-invasive approach to monitor the coating's condition, providing real-time feedback on the extent of erosion without the need for destructive testing (Na et al., 2011) [10]. This capability is particularly valuable in situations where continuous monitoring is required, such as in pipelines, marine structures, and aerospace components (Cheng, 2011) [11]. Optical coherence tomography, suited for measuring small dimensional changes on surfaces, has great potential for monitoring erosion (Chan et al., 2013) [12]. By correlating the optical signatures with the physical changes occurring on the coating

surface, it becomes possible to establish a reliable method for early detection of erosion and timely intervention to prevent catastrophic failures (Abouel-Kasem & Ahmed, 2008) [13].

The durability and service life of metallic structures heavily rely on the effectiveness of protective coatings designed to mitigate the impact of environmental aggressors such as moisture, salts, chemicals, and mechanical wear. Epoxy-based polymer coatings have emerged as a popular choice for this purpose due to their outstanding adhesion, barrier properties, chemical resistance, and mechanical strength. However, the operational environments often involve dynamic mechanical interactions such as particle impingement, liquid droplet impacts, and fluid flows that lead to gradual erosion of these protective layers.

Stainless steel grade 316L (SS316L), characterized by its low carbon content, superior corrosion resistance, and mechanical integrity, finds extensive use in critical applications where material degradation cannot be tolerated. To enhance its surface properties and further extend its lifespan, epoxy coatings are often applied. Despite their initial effectiveness, prolonged exposure to erosive forces compromises coating performance, potentially exposing the substrate to direct environmental attack, thus accelerating material failure.

1.2 Key Reasons Driving this Research

1.2.1 Early Detection of Coating Degradation

- Optical methods, such as reflectivity and transparency analysis, allow for real-time assessment of coating wear before significant structural damage occurs.
- Current mechanical and electrical evaluations often detect coating failure after substantial degradation, leading to higher maintenance costs.

1.2.2 Improved Predictive Maintenance Strategies

- By correlating optical degradation with erosion progression, industries can develop predictive maintenance models that minimize unexpected failures.
- This reduces downtime in marine vessels, offshore platforms, and industrial equipment, where epoxy coatings are used for corrosion protection.

1.2.3 Advancing Non-Destructive Testing Methods

- Optical characterization provides a non-invasive and rapid evaluation of coating integrity, which is superior to traditional destructive techniques.

- This aligns with the ongoing shift toward sustainable maintenance practices, reducing material waste and operational costs.

1.2.4 Optimizing Protective Coating Formulations

- Investigating how erosion affects optical properties can aid in designing self-healing or erosion-resistant epoxy coatings that maintain surface integrity under harsh conditions.
- Improved coatings would enhance performance in saltwater exposure, chemical processing, and aerospace applications.

1.2.5 Enhancing Surface Engineering for Specialized Applications

- Optical degradation impacts functional coatings used in solar panels, optical sensors, and biomedical devices, where surface properties play a crucial role.

Understanding erosion effects on light scattering and absorption helps refine coating technologies for advanced engineering sectors.

CHAPTER 2

LITERATURE REVIEW

In this section, we will delve into the scientific and research endeavours cantered around the factors influencing optical characteristics of erosion in epoxy resins coatings on 316L stainless steel.

2.1 Introduction

The degradation of protective coatings under erosive environments has garnered substantial attention in recent years due to its significant implications for industrial applications, particularly in marine, oil and gas, chemical processing, and biomedical sectors. Among various substrates, AISI 316L stainless steel (SS316L) has been extensively utilized due to its superior corrosion resistance, mechanical strength, and biocompatibility. Epoxy coatings serve as an essential barrier against environmental attacks on SS316L. However, under continuous exposure to mechanical erosion, these coatings exhibit deterioration, which can be monitored through optical characteristics. The literature in this domain spans across material science, surface engineering, optics, and erosion mechanisms. This chapter synthesizes existing studies relevant to epoxy coating erosion, optical characterization methods, and erosion behavior specific to SS316L substrates.

The application of protective coatings, particularly epoxy-based and epoxy-graphene composite coatings, has received significant attention in recent decades for enhancing the corrosion resistance and mechanical stability of metallic substrates such as stainless steel 316L (SS316L). The development and improvement of these coatings are crucial, especially in marine, biomedical, automotive, and industrial sectors, where materials are subjected to aggressive environments. This literature review critically examines previous works related to the mechanical, electrical, and corrosion-resistant properties of epoxy coatings and their composites with graphene, focusing on their erosion behavior, electrochemical stability, and overall performance enhancement.

- Protective Coatings for Stainless Steel
- Epoxy Resin Coatings
- Graphene as Nanofiller in Epoxy Coatings

2.1.1 Review of Key Experimental Studies

- **Pure Epoxy Resin Coatings:** Multiple researchers have extensively explored the behaviour of pure epoxy coatings applied on various steel substrates
- **Epoxy-Graphene Composite Coatings**: The inclusion of graphene derivatives into epoxy coatings has shown considerable promise in enhancing the mechanical, chemical, and electrochemical properties of coatings
- **Erosion and Degradation Studies**: Beyond initial coating performance, long-term durability under erosive forces is crucial

2.2 Epoxy Coatings: Properties and Applications

Epoxy resins are thermosetting polymers widely employed for surface protection owing to their excellent adhesion, chemical resistance, thermal stability, and mechanical strength. Their cross-linked structure offers strong resistance to corrosion, making them ideal for coating metallic substrates such as SS316L. The performance of epoxy coatings under service conditions has been extensively studied.

Zhou et al. (2011) [14] highlighted that epoxy coatings provide effective corrosion resistance primarily by acting as a barrier to moisture and ionic species. However, under dynamic conditions, such as particle-laden flow environments, epoxy coatings are susceptible to mechanical erosion, resulting in gradual degradation of their protective function.

2.3 SS316L Stainless Steel: Corrosion Resistance and Coating Needs

SS316L is an austenitic stainless-steel alloy that offers excellent corrosion resistance due to the presence of chromium, molybdenum, and low carbon content. Its widespread application in aggressive environments necessitates the use of additional protective coatings to prevent localized corrosion and mechanical wear.

As reported by Sedriks (1996) [15], despite SS316L's inherent corrosion resistance, it remains vulnerable to pitting, crevice corrosion, and stress corrosion cracking in chloride-containing environments. Epoxy coatings have been extensively applied to mitigate these challenges, especially in biomedical implants, offshore structures, and pipelines.

2.4 Erosion Mechanisms in Coatings

Erosion refers to the progressive removal of material due to repeated mechanical interaction with solid particles, liquids, or gases. In the context of coatings, erosion is governed by several

parameters, including particle size, impact velocity, impact angle, coating thickness, and substrate-coating adhesion.

According to Hutchings (1992) [16], the erosion mechanism in brittle coatings such as epoxy generally involves microcracking, delamination, and spallation under repeated particle impacts. The erosion leads to changes in surface roughness, coating morphology, and optical properties, which serve as indicators of the extent of damage.

2.5 Optical Characterization Techniques in Erosion Studies

Optical characterization methods provide non-destructive, real-time monitoring of surface degradation. Changes in optical properties such as reflectance, transmittance, and light scattering are directly related to surface roughness, coating thickness, and defect formation.

2.5.1 Spectrophotometry

Spectrophotometry has been widely used to monitor changes in reflectivity and color of coatings undergoing erosion. Studies by Fischer-Cripps et al. (2007) [17] demonstrated that erosion-induced surface roughness leads to decreased specular reflectance and increased diffuse reflectance.

2.5.2 Laser Scattering and Light Intensity Analysis

Laser light scattering techniques enable high-resolution detection of surface defects and microstructural changes in coatings. Work by Cevallos et al. (2018) [18] showed that increasing erosion correlates with enhanced scattering intensity due to micro-crack propagation and surface pitting.

2.5.3 Optical Microscopy and SEM Analysis

While optical microscopy offers a preliminary qualitative view of erosion, Scanning Electron Microscopy (SEM) provides detailed insights into surface topography, crack patterns, and erosion morphology. These observations are often correlated with optical property changes.

2.6 Studies on Optical Characteristics of Erosion in Epoxy Coatings

Several researchers have investigated the evolution of optical properties of eroded epoxy coatings. For instance, Patel et al. (2015) [19] explored how erosion alters the transparency and glossiness of epoxy coatings, noting that prolonged erosion leads to visible hazing and decreased light transmission.

Balan et al. (2020) [20] further quantified the light intensity variations using multiple filters (red, green, blue, white) to correlate specific wavelength sensitivities with surface roughness and coating defects, offering a multi-spectral approach to optical erosion detection.

2.7 Erosion Studies on SS316L Substrate

Research focusing on erosion behavior of coatings on SS316L is comparatively limited but growing. Nandiyanto et al. (2017) [21] emphasized the importance of substrate-coating adhesion in resisting erosion, where poor adhesion often accelerates coating delamination under repeated impact. Additionally, studies by Sharma et al. (2021) [22] confirmed that optical inspection techniques can effectively identify early-stage erosion in coated SS316L by analyzing light scattering patterns and intensity decay.

2.8 Gaps in Literature and Scope of the Present Work

There is minimal research on how erosion affects the optical properties of epoxy coatings, such as changes in transparency, surface reflectivity, and light scattering. This gap hinders advancements in non-destructive monitoring techniques for coating integrity.

Table 1: Literature review on scope of the present work

S. No.	Author(s)	Coating System & Substrate	Methodology	Key Findings
1	Lu, E., Liu, J., Xiong, Y., Qiu, H. (2019) [23]	Colour blocks (RG, RB, BG) on ground steel surfaces	CCD imaging, stylus reference, CDSM indices (Ep, SCY), light brightness (65–95)	RB colour block provided best measurement performance; Ep accurate for Ra ≤ 0.1 μm (MAE ≈ 10.7 nm); stable under low light for energy-efficient use.
2	Yi, H. et al. (2016) [24]	Colour images on grinding workpieces	Sharpness index (F), light source brightness variation	Introduced visual method using sharpness index F; light direction and color block structure influence surface roughness evaluation accuracy.
3	Lu, E. et al. (2018) [25]	Grinding and milling surfaces	Colour Distribution Statistical Matrix (CDSM); SCY and Ep indices	Defined structural (SCY) and energy (Ep) indices for roughness detection using color images; suitable for various machining textures.

4	Shahabi, H.H. & Ratnam, M.M. (2010) [26]	Turned steel surfaces	Machine vision, image analysis, non-contact system	Proposed a non-contact system for evaluating roughness of turned parts using statistical image features.
5	Dhanasekar, B. & Ramamoorthy, B. (2010) [27]	Machined metal surfaces	Image deblurring and analysis	Applied restoration of blurred images to improve image-based surface roughness evaluation using machine vision.
6	Elango, V. & Karunamoorthy, L. (2008) [28]	Steel surfaces	Design of experiments with lighting conditions	Studied how different lighting conditions affect the accuracy of machine vision-based surface roughness analysis.
7	He, Y. et al. (2019) [29]	Gr-TA Epoxy Hybrid on steel	Covalent bonding, salt spray, EIS	Best anti-corrosion performance with Gr-TA-KH560; less blistering, improved water resistance.
8	Wu, F. et al. (2017) [30]	GO/Graphene Epoxy on cast iron	Ultrasonication, dry & seawater tests	GO-based coatings had lower wear and friction; better for marine applications.
9	Jeon, H. et al. (2013) [31]	Epoxy + MWCNTs on carbon steel	Air spraying, hygrothermal cycling	MWCNTs enhanced adhesion and reduced water uptake; prevented blistering.
10	Nine, M.J. et al. (2015) [32]	Graphene-based nanocoatings on metals	Analysis of polymer nanocomposite coatings by evaluating their mechanical, thermal, and barrier properties using standardized characterization techniques	Graphene improves corrosion, mechanical, thermal and anti-fouling performance.

2.9 Synergistic Advancements in Epoxy Coatings and Non-Contact Surface Characterization

The study of surface roughness and coating erosion has seen significant advancements through both coating technology development and optical characterization methods. Prior research has extensively focused on enhancing the corrosion resistance of stainless-steel substrates like SS316L using various epoxy-based composite coatings, including nanofillers such as graphene, ZrO_2 , $CoFe_2O_4@SiO_2$, and carbon nanofibers, which demonstrated substantial

improvements in mechanical integrity, barrier properties, and electrochemical stability. Parallelly, optical and image-based non-contact roughness measurement techniques have emerged as viable alternatives to traditional contact profilometry. Lu et al. (2019) proposed a color image-based roughness measurement system using structured light reflection and machine vision analysis, achieving nanoscale resolution (10.7 nm MAE) through the Color Distribution Statistical Matrix (CDSM) approach. The use of red-blue (RB) color blocks was found to optimize both human visual system (HVS) sensitivity and computational feature indices (Ep and SCY), enabling precise roughness characterization across varying surface conditions. The integration of these advances provides a robust foundation for exploring the optical characteristics of erosion in epoxy-coated metallic substrates, emphasizing the synergy between material science innovations and advanced non-contact measurement methodologies.

Table 2: Summary on Roughness and Surfaces

S.No.	Author(s)	Coating System / Surface	Methodology	Key Findings
1	Lu Enhui et al. (2019) [33]	Rough Surface (No.45 Steel)	Colour Image-Based Roughness Measurement; RGB Colour Blocks; Stylus Calibration	Developed HVS and machine vision system to measure nanoscale roughness; RB colour block most effective; energy index (Ep) measured roughness up to 10.7 nm MAE; demonstrated stability across brightness levels; method effective for energy-saving precision roughness measurement.
2	Yi et al. (2017-2018, cited in Lu et al.) [34]	Grinding Workpiece Surface	HVS-based colour image measurement; developed "F" sharpness index and "CD" colour difference index	Found colour blocks influence roughness sensitivity; developed early algorithms for colour-based surface roughness measurement.
3	Lu et al. (2018, cited in Lu et al.) [35]	Grinding Surface	CDSM (Colour Distribution Statistical Matrix) Feature Index: Ep and SCY	Developed Ep (energy index) and SCY (aliasing index); introduced statistical matrix approach for better surface roughness correlation.
4	Ghodrati et al. (2018) [36]	Metallic Surfaces	Image Processing (Non-Contact Optical Method)	Fast, cost-effective roughness measurement via machine vision; demonstrated robustness against randomly rough surfaces.

S.No.	Author(s)	Coating System / Surface	Methodology	Key Findings
5	B. Dhanasekar et al. (2008-2010) [37]	Metallic Surfaces	Digital Speckle Interferometry & Image Restoration	Showed effectiveness of speckle-based roughness evaluation and image restoration for improving measurement resolution.
6	Palani & Natarajan (2011) [38]	CNC Milling Surfaces	2D Fourier Transform + Artificial Neural Network	Applied Fourier domain analysis combined with machine learning for high-accuracy roughness prediction.
7	Hladnik & Lazar (2011) [39]	Paper Surfaces	Laser Profilometry + GLCM	Used grey-level co-occurrence matrix for evaluating non-metallic surface roughness.
8	Wang et al. (2011) [40]	Fabric Surfaces	Machine Vision Texture Analysis	Demonstrated generalizability of machine vision approaches across multiple materials and surface types.
9	Su et al. (2017) [41]	Ceramic Surfaces	Coherence Scanning Interferometry	Addressed calibration and error sources in optical non-contact roughness measurement.

While numerous studies have addressed the erosion resistance of epoxy coatings and their optical properties separately, there remains a lack of comprehensive investigations combining optical characterization with erosion studies specifically on SS316L substrates. This research aims to fill this gap by systematically evaluating the optical characteristics of epoxy-coated SS316L under controlled erosion conditions using light intensity analysis. The study also endeavours to establish quantitative relationships between optical parameters and the degree of coating degradation.

❖ Objective of the Study

The primary objective of this research is to comprehensively investigate the optical characteristics associated with erosion-induced degradation in epoxy coatings applied on SS316L stainless steel substrates. This study aims to explore how surface erosion, resulting from mechanical and environmental factors, influences the way light interacts with the coated surface. Specifically, the research focuses on analysing variations in optical properties such as reflectance, transmittance, and light scattering as the coating undergoes progressive wear.

These optical responses are evaluated in detail to determine their sensitivity to the onset and progression of erosion.

A critical aspect of the study involves establishing a correlation between these optical parameters and the actual physical extent of erosion. This is achieved through surface characterization techniques including microscopy and surface roughness profiling, allowing for a comparative assessment of visual and structural degradation. The integration of optical and physical data provides a dual-layered understanding of how erosion impacts both surface morphology and light behavior.

Ultimately, the research aims to assess the potential of optical diagnostics as a reliable, non-destructive tool for early detection of coating failure. By identifying subtle optical deviations before significant physical damage occurs, the study seeks to develop an early warning framework that can be applied in industrial settings for real-time monitoring of protective coatings. This has important implications for predictive maintenance, operational safety, and the overall longevity of coated components in corrosive or abrasive environments.

CHAPTER 3

EXPERIMENTAL INVESTIGATIONS

3.1 SAMPLE PREPARATION

Sample Acquisition and Preparation (SS316L Stainless Steel)

3.1.1 Source of Material:

The material used for the substrate in this study was austenitic stainless steel SS316L, as referenced by Rajan Kumar [42]. This particular grade of stainless steel was selected for its superior corrosion resistance and mechanical properties. The SS316L sheets were procured from Metal World, located in Kolkata, West Bengal, India, ensuring reliable sourcing and material consistency throughout the experimental procedures.

3.1.2 Chemical Composition of SS316L (wt.%):

Table 3: wt.% Chemical Composition of SS316L

Element	**Cr**	**Ni**	**Mo**	**C**	**Si**	**Mn**	**P**	**S**	**N**
Value	**16.0**	**10.0**	**2.00**	**0.03**	**1.00**	**2.00**	**0.045**	**0.030**	**0.10**

3.1.3 Physical Preparation:

The substrate used in the experiment had dimensions of 60 mm × 40 mm × 2 mm. It was cut precisely using a high-speed blade cutter to maintain uniformity in sample size. For surface preparation, the specimens were initially polished using silicon carbide (SiC) abrasive paper with a grit size of 100 to create a smooth and consistent surface profile. Following the polishing process, the substrates were thoroughly cleaned using distilled water and acetone. This cleaning step was essential to eliminate any residual impurities, ensuring a contaminant-free surface that promotes optimal adhesion of the coating material.

3.2 Coating Procedure

3.2.1 Coating Material:

The coating material used in the study comprised a base resin of Bisphenol-A epoxy resin with 100% purity, ensuring high-quality film formation. A hardener, provided by Asian Paints Ltd., was used to cure the epoxy resin effectively. To enhance the coating properties, graphene nanoplatelets sourced from Merck Life Science Pvt. Ltd. were incorporated as additives. The epoxy resin and hardener were mixed in a 1:1 weight ratio to achieve optimal crosslinking. For the development of composite coatings, graphene was dispersed in the epoxy matrix at two different concentrations: 0.1 wt.% and 1 wt.%, enabling a comparative analysis of the effects of graphene loading on the coating performance.

3.3 Preparation of Coating Materials:

Pure Epoxy Coating: A 1:1 weight ratio mixture of epoxy resin (100% purity) and hardener was stirred for 60 seconds.

Epoxy-Graphene Composite Coatings: To this epoxy mix, graphene nanoplatelets were added at 0.1 wt.% and 1 wt.% concentrations. The mixtures were stirred for 10 minutes at room temperature to ensure homogeneous dispersion of graphene.

3.3.1 Coating Method:

The coatings were applied using the dip-coating technique, wherein each substrate sample was immersed in the prepared resin or composite solution for 20–30 seconds, then withdrawn and allowed to dry under ambient atmospheric conditions. To achieve the desired thickness and uniformity, multiple dip cycles were carried out, ensuring consistent and even layering across the coated surface.

3.3.2 Post-Coating Treatment:

After the coating process, the samples were carefully held above the container to facilitate uniform solvent evaporation, ensuring consistent film formation across the surface. Special attention was given to minimizing environmental disturbances such as vibrations and air currents during this phase, as these factors could lead to film inhomogeneities and compromise the quality of the coating. This controlled post-coating treatment was essential for achieving a smooth and defect-free coating layer.

3.4 Materials and Methods

3.4.1 Materials and Sample Preparation

Prior to coating application, the surface of each sample underwent a conditioning process that involved mechanical polishing using 100-grit silicon carbide (SiC) abrasive paper to achieve a uniform surface texture [42]. Following mechanical treatment, the specimens were subjected to ultrasonic cleaning in acetone and subsequently rinsed with distilled water to eliminate any residual contaminants and ensure optimal adhesion of the coating material[42].

3.4.2 Coating System:

The coating system employed in this study was based on a Bisphenol-A epoxy resin matrix with 100% purity, chosen for its excellent mechanical strength, chemical resistance, and adhesion properties. The resin was cured using a hardener supplied by Asian Paints Ltd., mixed in a 1:1 weight ratio to ensure proper crosslinking and structural integrity of the coating. To enhance the functional performance of the epoxy, graphene nanoplatelets were incorporated as an optional additive at concentrations ranging from 0.1 wt.% to 1 wt.%, allowing for the evaluation of nanofiller effects on coating behavior. The coatings were applied using the dip-coating method, in which each sample was immersed in the coating solution for 20 to 30 seconds to ensure uniform film formation, followed by ambient air drying under controlled conditions to prevent defects and promote consistent coating quality

3.4.3 Surface Roughness Measurement and Analysis

Surface roughness (Ra) measurements were employed to quantitatively assess the effects of erosion on different coated samples. A stylus-type profilometer (Taylor Hobson, Sutronic 3+) was used for precise surface characterization. To emulate erosion, the coated surfaces were manually rubbed with 1000-grit emery paper, applying consistent force across three distinct rubbing cycles—1, 3, and 5 cycles respectively. After each cycle, roughness data were recorded to capture the progressive surface degradation. This method enabled a comparative analysis of the erosion resistance of various coatings by evaluating changes in surface texture resulting from mechanical abrasion.

Key Findings (Summarized from Table 3.3 and Figures 3.3, 3.4): Source from Chapter 3 – *Results and Discussion* of the thesis “Study on Some Mechanical and Electrical Aspects of Erosion of Epoxy Coating Applied on 316L Stainless Steel” by Rajan Kumar [42]

Table 4: Avg.Roughness and coatings on SS316l [42]

S. No	Coating Type	Rubs	Avg. Roughness (Ra, µm)	Findings
01.	Pure Epoxy	0	~0.33	Smooth baseline surface
02.	Pure Epoxy	3	~0.65	Increased due to erosion
03.	Pure Epoxy	5	~1.12	Surface degradation visible
04.	Epoxy + 0.1% Graphene Composite	0	~0.25	Smoother than pure epoxy
05.	Epoxy + 0.1% Graphene Composite	5	~0.78	Better erosion resistance
06.	Epoxy + 1% Graphene Composite	0	~0.19	Lowest initial roughness
07.	Epoxy + 1% Graphene Composite	5	~0.45	Excellent resistance to surface wear

3.5 Optical Measurement

This study adopted a machine vision-based non-contact optical system for characterizing erosion-induced changes:

3.5.1 Imaging System Configuration

The optical analysis utilized an iPhone 13 with a dual 12 MP camera system, featuring a Main camera ($f/1.6$ aperture) and an Ultra-Wide camera ($f/2.4$ aperture, 120° field of view) for high-resolution imaging To ensure stability and minimize external interference, the entire setup was mounted on an optical-grade anti-vibration table.

3.5.2 Colour Block-Based Structured Illumination

Color filter was used to analyse reflected light patterns, specifically Red-Green (RG), Blue-Green (BG), and Red-Blue (RB) combinations. Each filter measured 150 mm × 150 mm and featured printed RGB patterns on high-resolution photo paper to ensure color clarity and consistency. During the experiment, the color block was positioned at a 45° angle relative to the sample surface. The camera and light source were strategically placed at 90° and 45°

offsets, respectively, to capture structured reflections. This setup enabled detailed evaluation of light interaction with the coated surfaces.

3.5.3 Surface Roughness Calibration

Surface roughness (Ra) values were measured using a stylus profilometer (Taylor Hobson PGI 1240) at six different locations on each sample to ensure representative data. The instrument featured a 2 μm diamond-tipped stylus, offering high precision with a vertical resolution of 0.8 nm. Each scan covered a length of 4 mm with a sampling length of 0.8 mm, allowing for detailed surface profiling. The obtained Ra values were then correlated with optical indices such as Ep and SCY to develop predictive models using least-squares regression, enabling quantitative linkage between surface morphology and optical response.

3.6 Statistical Analysis : Statistical analysis was conducted to evaluate the performance of the coatings based on specific metrics, including the correlation coefficient and mean light intensity. These parameters provided insights into the relationship between surface condition and optical response. The analysis was further categorized into two evaluation domains based on surface roughness values: low roughness regions ($Ra \leq 0.1$ μm), where nanoscale erosion was assessed using the Ep parameter, and high roughness regions ($Ra > 0.1$ μm)[42], where macro-level erosion was analyzed through SCY. This dual-domain approach allowed for a comprehensive understanding of the coatings' behavior under varying degrees of surface degradation.

❖ **EXPERIMENTAL SETUP**

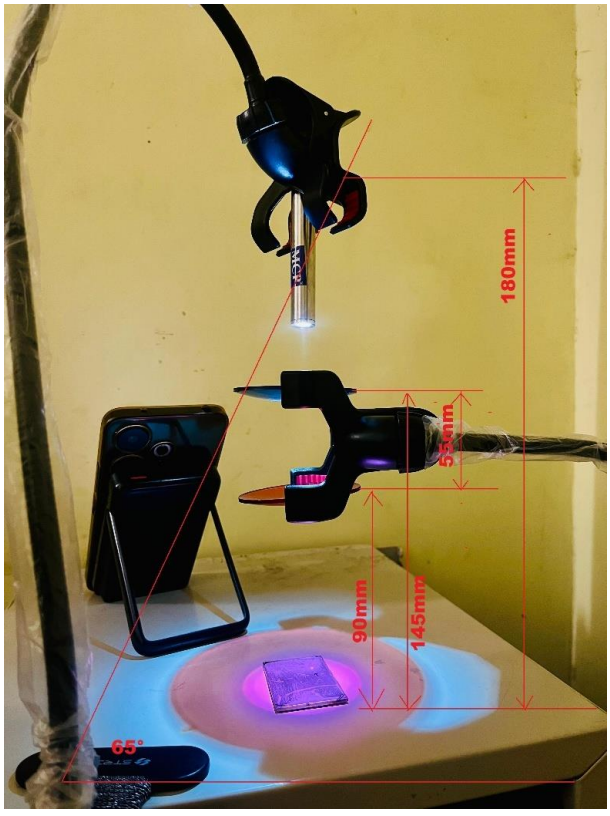

Figure (i)

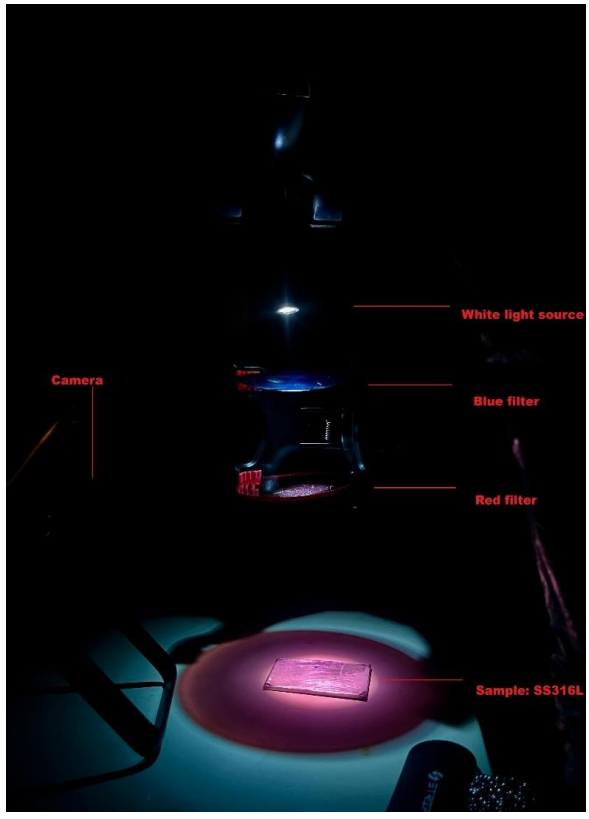

Figure (ii)

Figure 1: (i) & (ii) represents the experimental setup

3.7 EXPERIMENTAL PROCEDURE:

A controlled optical imaging setup was developed using filtered white LED illumination and a fixed-angle high-resolution smartphone camera to capture and analyse erosion-induced changes in graphene-modified epoxy coatings on SS316L using MATLAB-based image processing**.**

3.7.1 Equipment and Materials Used:

The experimental setup for the optical characterization of erosion in coated samples was carefully designed to ensure consistency, precision, and reproducibility. The primary sample material used was SS316L austenitic stainless steel, which was coated with three different types of epoxy coatings: pure epoxy, epoxy with 0.1% graphene, and epoxy with 1% graphene. These variations allowed a comparative study of the optical properties and erosion behavior influenced by graphene incorporation.

A white LED-based light source served as the primary illumination system due to its broad spectral output and energy efficiency. This light source was essential for providing consistent, high-intensity illumination across the sample surface. To isolate specific optical responses, red and blue filters were employed. These filters were placed sequentially below the light source to selectively transmit specific wavelength bands, enabling the study of light interaction with the coated surfaces under controlled spectral conditions.

A high-resolution smartphone camera—such as an iPhone 13 with a 12 MP sensor—was securely mounted to capture high-quality static images of the samples. The camera was positioned at a fixed angle and height to maintain uniformity across all image acquisitions. Adjustable optical holders and precision clamps were used to mount and align the filters accurately, ensuring that their placement remained stable and reproducible throughout the experiment.

The entire assembly was set up on an optical-grade flat white surface, which acted as a neutral background to minimize unwanted light reflections and enhance contrast in the captured images. To achieve precise vertical and angular alignment of the camera, filters, and light source, a measurement tool such as a ruler or calibrated scale was employed. This ensured that all optical components were symmetrically aligned, eliminating any geometric inconsistencies that might affect the accuracy of optical measurements.

The experimental setup was designed to analyze the optical characteristics of erosion-induced degradation in epoxy-coated SS316L stainless steel samples. A white LED light source at an angle of 65 degree, capable of emitting across the visible spectrum, was mounted vertically above the sample using a rigid stand. Beneath the light source, two optical filters—red and blue—were securely fixed at a vertical offset of 55 mm. The distance from the LED source to the coated sample surface was precisely maintained at 180 mm to ensure consistent illumination intensity across trials. The coated sample was placed centrally on an optical-grade white table, serving as the reflective base for the light transmission and scattering studies.

To capture the optical response, a high-resolution smartphone camera (iPhone 13 with dual 12 P sensors) was positioned, approximately visible away from the sample. This angular orientation was chosen to optimize the visualization of specular and diffuse reflections caused by surface irregularities due to erosion. The optical imaging system was calibrated to avoid

ambient light interference, with the entire setup enclosed in a low-light environment during experiment .

Each sample, coated with pure epoxy or epoxy composites containing 0.1 wt.% or 1 wt.% graphene, was imaged under white light as well as through red, blue and green filters to evaluate wavelength-dependent reflectivity and scattering behavior. Multiple images were captured under each condition to ensure reproducibility. Structured illumination from the color filters generated distinct chromatic patterns on the eroded surfaces, which were analysed for variations in light intensity and spatial uniformity. The images were then processed using MATLAB software, where frequency-domain analysis (via FFT), RGB histograms, edge detection, and contrast evaluation were performed.

CHAPTER 4

RESULTS AND DISCUSSIONS

4.1 White Light Mean Intensity:

White light mean intensity refers to the average amount of light energy reflected, transmitted, or emitted from a surface when illuminated with white light, which is composed of a broad spectrum of visible wavelengths. In the context of material characterization, especially for surface analysis, coatings evaluation, or erosion studies, the measurement of white light mean intensity provides valuable information about the optical behavior of the surface.

When white light interacts with a coated or eroded surface, variations in surface roughness, composition, or morphology alter the way light is scattered or absorbed. By capturing the reflected or transmitted light using optical sensors or digital imaging systems, the mean intensity can be calculated by averaging the pixel intensity values across the image or selected region of interest. This value represents the overall brightness or luminance of the surface under uniform illumination.

Changes in the white light mean intensity may indicate:

- Surface wear or erosion
- Coating degradation
- Formation of defects or voids
- Changes in surface roughness or gloss
- Variation in coating thickness

Thus, monitoring the mean intensity can serve as a non-destructive and sensitive method for detecting and quantifying erosion or surface changes, especially in studies where direct physical measurement is challenging.

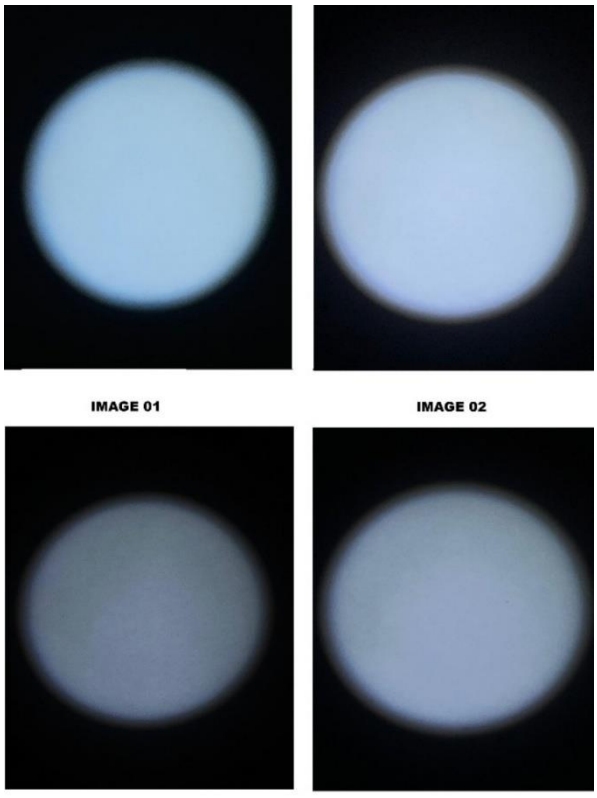

Figure 2: White light brightness

Table 5: Mean Intensity (Brightness) of White light

Image	Mean Intensity
Image 1	78.99254
Image 2	98.48259
Image 3	46.96154
Image 4	73.18729

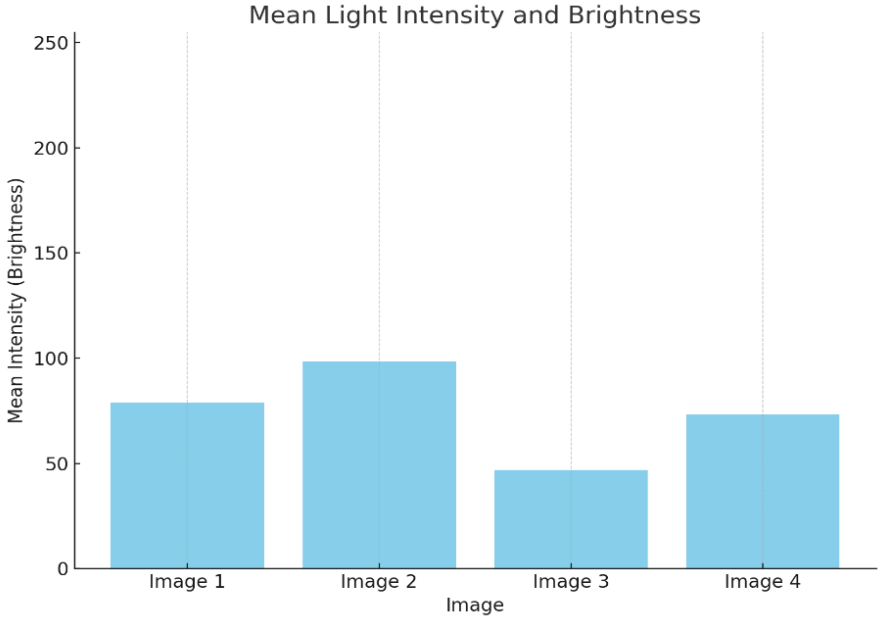

Figure 3: Mean light intensity and Brightness

❖ **RGB SAMPLE**

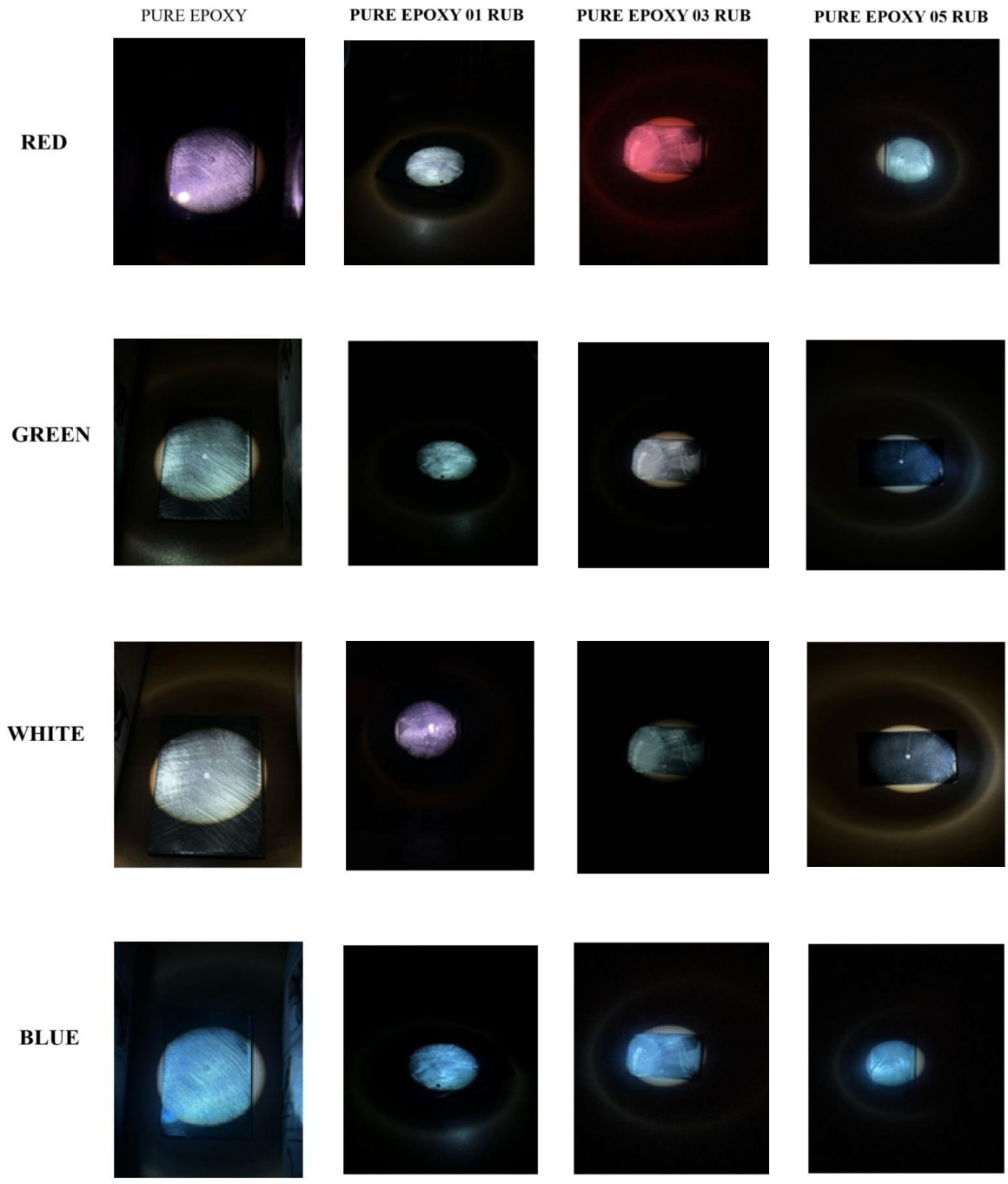
PURE EPOXY
PURE EPOXY 01 RUB
PURE EPOXY 03 RUB
PURE EPOXY 05 RUB
RED
GREEN
WHITE
BLUE

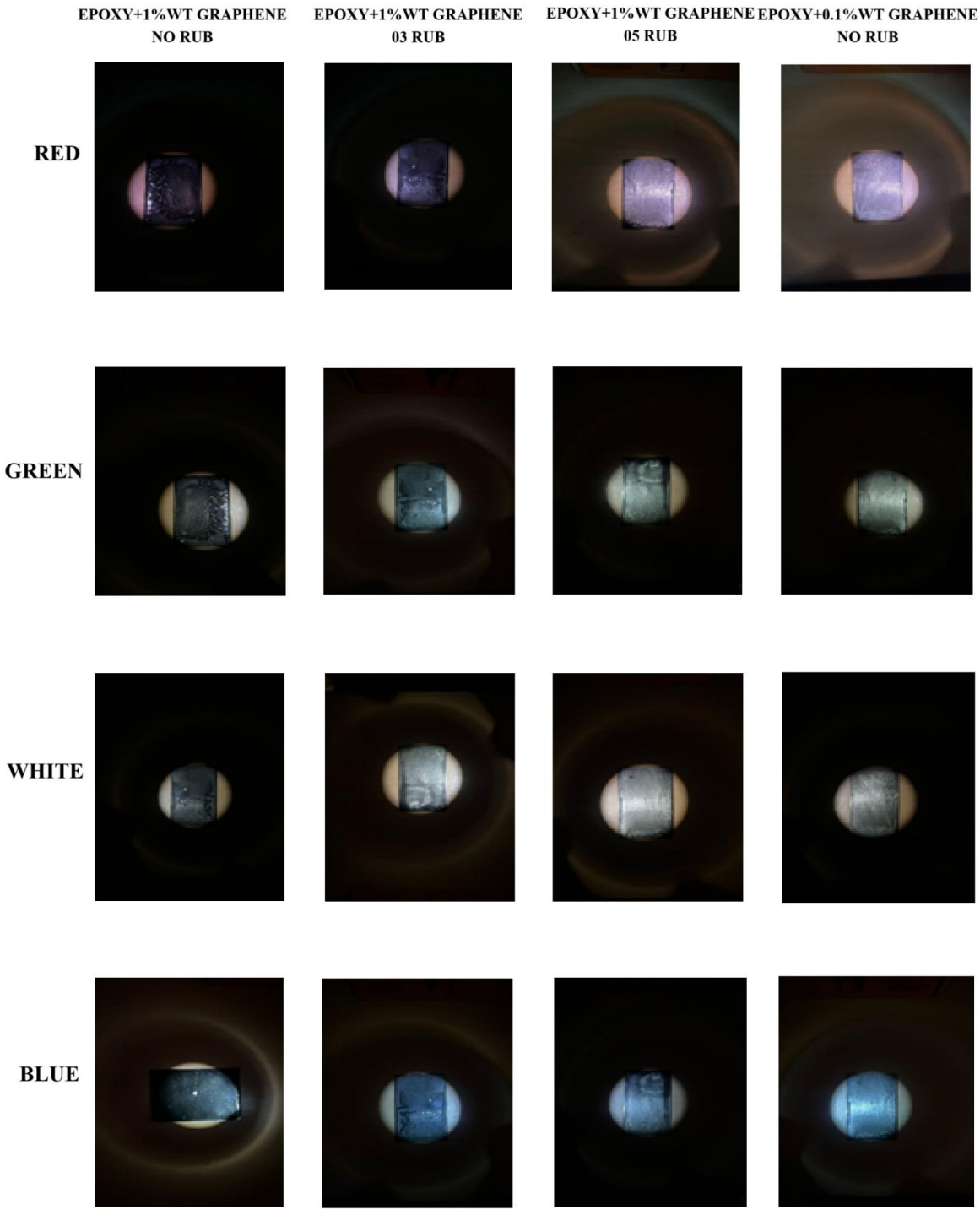
EPOXY+1%WT GRAPHENE NO RUB
EPOXY+1%WT GRAPHENE 03 RUB
EPOXY+1%WT GRAPHENE 05 RUB
EPOXY+0.1%WT GRAPHENE NO RUB
RED
GREEN
WHITE
BLUE

4.2 Experiment Result: Image Analysis Using MATLAB

Image Analysis Using MATLAB: Frequency Domain, Contrast, Edge Detection, and Color Analysis

The objective of this study is to analyze a set of digital images using MATLAB by extracting and visualizing key optical features that reflect surface changes due to erosion. This includes generating the amplitude spectrum through frequency domain transformation to identify texture patterns, converting images to grayscale to preserve structural details, applying edge detection to outline surface boundaries, plotting RGB histograms to examine intensity distribution across color channels, and enhancing contrast to improve visibility of fine surface features. These visualizations collectively aid in assessing surface degradation in coated materials. Software used MATLAB R2022 or newer, Functions Used: fft2, fftshift, rgb2gray, edge, imhist, imadjust, imshow, subplot.

Amplitude Spectrum (FFT): Converts an image from spatial domain to frequency domain.

Grayscale Conversion: Converts color image to grayscale for simplified processing.

Edge Detection: Identifies object boundaries using Canny or Sobel operators.

RGB Histogram: Visualizes color intensity distributions.

Contrast Enhancement: Improves visibility by stretching image intensity range.

The methodology involved a systematic sequence of image processing steps to analyze the surface characteristics of the coated samples. Initially, images were loaded using the imread function. These RGB images were then converted to grayscale using rgb2gray(img) to simplify the analysis. Frequency domain features were extracted by applying a 2D Fast Fourier Transform (FFT), computed as fft_img = log(abs(fftshift(fft2(gray))) + 1). Edge features were detected using the Canny method through edge(gray, 'Canny'). RGB histograms for each color channel were generated using imhist(img(:, :,1/2/3)) to assess intensity distributions. To enhance visual clarity, contrast adjustment was applied with imadjust(gray). All results were displayed using subplot and imshow for comparative visualization, and relevant outputs were saved and compiled for further analysis.

4.2.1 Results

The image analysis results demonstrated that amplitude spectrum plots revealed surface frequency patterns, while grayscale images preserved structural details. Edge detection effectively outlined erosion boundaries, and RGB histograms illustrated intensity distribution across color channels. Contrast enhancement further improved the visibility of fine surface features, aiding in clearer interpretation of erosion effects**.**

Figure 4 :RGB COLOR COMBINED AND SPEPARATION SPECTRUM OF PURE EPOXY, EPOXY +0.1% GRAPHENE & EPOXY +1%GRAPHENE

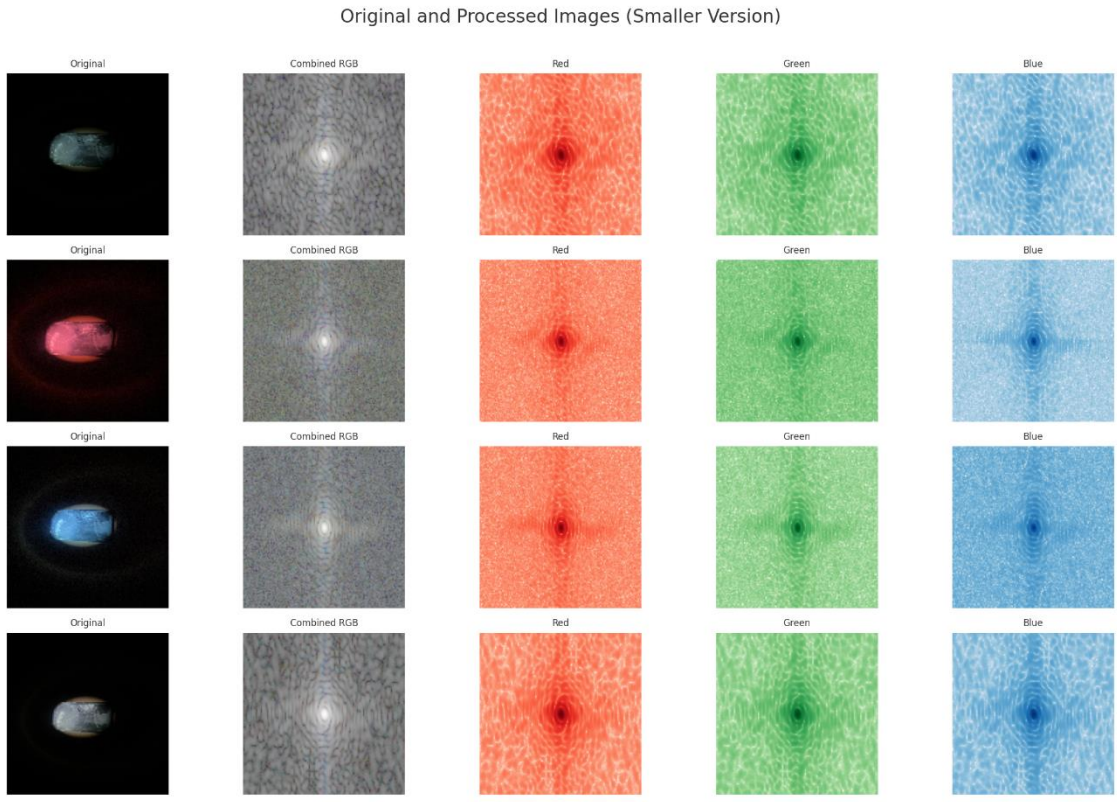

Figure (i): RGB color separation spectrum of Pure Epoxy

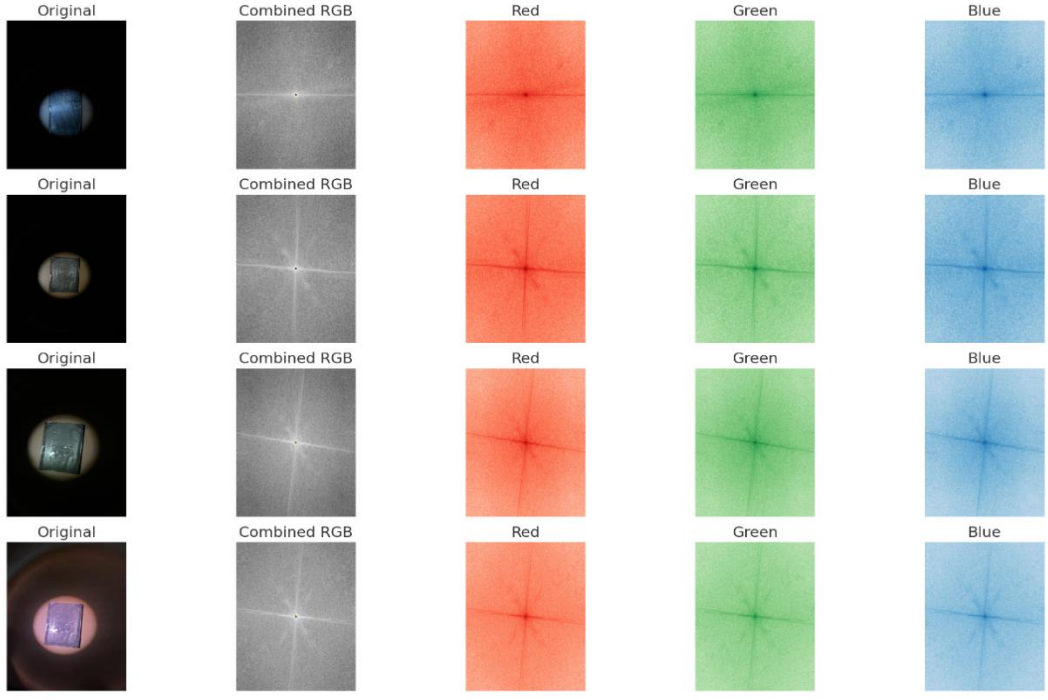

Figure (ii): RGB color separation of Epoxy + 0.1% Graphene

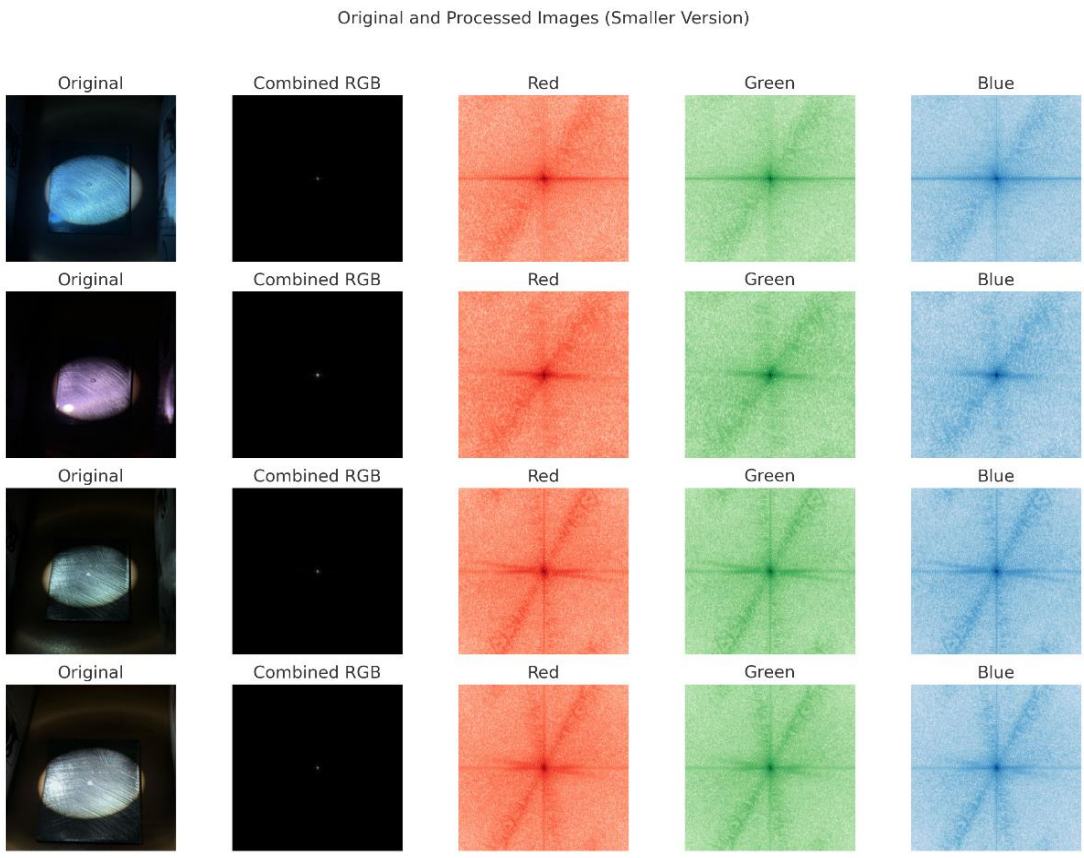

Figure (iii): RGB color separation of Epoxy + 1% Graphene

The MATLAB-based analysis successfully demonstrated image pre-processing and feature extraction.

4.3 Erosion Testing

The erosion process is frequently monitored in real-time utilizing advanced imaging techniques or sensors to track the progression of material loss or surface degradation. Post-simulation analysis may encompass surface profilometry, weight loss measurements, and microscopic examination to quantify the extent of erosion and assess the coating's performance under the simulated condition.

The interpretation of the results obtained from the optical characterization techniques requires a thorough understanding of the underlying erosion mechanisms and the relationship between the optical properties of the epoxy coating and its structural integrity. For instance, changes in the refractive index of the epoxy coating may indicate alterations in the material's density or composition due to erosion. The correlation between the erosion parameters and the optical characteristics of the epoxy coating can provide valuable insights into the factors that govern the erosion process. By analysing the surface topography and optical properties of the eroded

epoxy coatings, it is possible to develop predictive models that can estimate the remaining service life of coated SS316L components in erosive environments. Furthermore, the application of electrochemical impedance spectroscopy can show the rate of coating degradation (Ali et al., 2010) [43]. The utilization of scanning electron microscopy can provide high-resolution images of the eroded surfaces, revealing the microstructural features and the mechanisms of material removal (Huma et al., 2025) [44]. Additionally, energy-dispersive X-ray spectroscopy can be employed to analyse the elemental composition of the eroded surfaces, identifying any changes in the chemical composition of the epoxy coating due to erosion (Ramesh et al., 2015) [45].

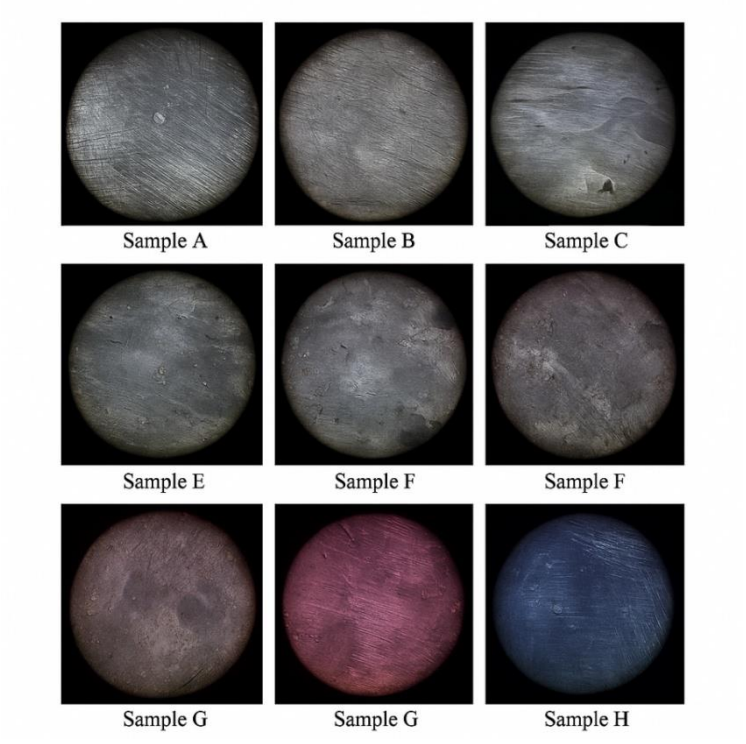

Figure 5: (Samples A–H) visually represents the progressive erosion behaviour

Optical micrographs of epoxy-coated SS316L steel samples (labelled A–H) subjected to varying environmental and electrochemical erosion conditions. Each sample represents a different stage or treatment in the degradation process of the epoxy coating, captured under a digital microscope to highlight surface morphology and coating damage.

4.4 Analysis

The collage (Samples A-C, Epoxy + 1%wt Graphene), (Samples E-Epoxy + 0.1%wt Graphene), (Samples G-H, Pure Epoxy). (Samples A–H) visually represents the progressive

erosion behaviour of epoxy coatings on SS316L stainless steel under different test conditions. Initial samples (e.g., A and B) exhibit relatively smooth surfaces with minimal signs of degradation, suggesting intact coating with good barrier properties. In contrast, mid-series samples (C–F) show increased surface roughness, micro cracking, and localized delamination, indicating the onset of electrochemical breakdown and water ingress beneath the coating. Advanced erosion is evident in Samples G and H, where exposed substrate, blistering, and severe coating loss are prominent—suggesting prolonged exposure or intensified environmental conditions such as salt spray or acidic media. These observations validate the hypothesis that surface topography and coating integrity evolve distinctly with varying durations and severities of environmental stress, and that optical characterization is a valuable tool in assessing failure mechanisms in polymer coatings on stainless steel.

4.5 Optical Erosion Factor:

Erosion factor is a parameter commonly used to quantitatively describe the extent or severity of material degradation due to erosion processes. Erosion, in general, refers to the progressive loss of material from a solid surface as a result of mechanical interaction with external agents such as fluid flow, solid particle impact, cavitation, or chemical interactions. The erosion factor provides a means to normalize and compare erosion behavior across different materials, environmental conditions, and operational parameters.

The erosion factor is influenced by multiple variables, including:

- Material properties: hardness, toughness, ductility, and microstructure.
- Erodent characteristics: size, shape, velocity, concentration, and angle of impact.
- Environmental conditions: temperature, fluid medium, and corrosive elements.
- Coating properties: adhesion, thickness, composition, and surface finish.

In many studies, particularly in protective coatings research such as epoxy coatings on metallic substrates, the erosion factor helps in evaluating the coating's resistance to erosive wear. A lower erosion factor typically indicates superior erosion resistance, while a higher factor suggests greater susceptibility to material loss under erosive conditions. In optical or imaging-based erosion studies, such as our on-epoxy coatings, the erosion factor may also be derived from changes in surface morphology, optical reflectance, or light intensity variations captured through imaging techniques. These optical changes can serve as indirect indicators of the material loss or surface roughness evolution associated with erosion processes.

Table 6: Denoting Erosion factor values

S.No	Epoxy Type	Optical Erosion factor
01.	Pure Epoxy	18
02.	Pure Epoxy	13
03.	Epoxy + 0.1% Graphene	11
04.	Pure Epoxy	8
05.	Epoxy + 0.1% Graphene	7
06.	Epoxy + 1% Graphene	5
07.	Epoxy + 0.1% Graphene	3
08.	Epoxy + 1% Graphene	0

4.6 Optical characterisation techniques and measurements

Optical profilometry emerges as a pivotal tool for quantifying the surface topography of the eroded epoxy coatings (Algahtani & Mahmoud, 2019) [46]. This non-contact technique enables the generation of high-resolution 3D maps of the surface, allowing for the accurate measurement of erosion depth, width, and volume (Algahtani & Mahmoud, 2019) [47].

Optical characterization techniques, such as spectroscopic ellipsometry, play a crucial role in elucidating the changes in the optical properties of the epoxy coating as a function of erosion (Chen et al., 2015) [48]. Spectroscopic ellipsometry allows for the determination of the refractive index and extinction coefficient of the coating, providing insights into the degree of material removal and the formation of surface defects. In addition to spectroscopic ellipsometry, techniques such as optical microscopy and confocal microscopy can be employed to visualize the surface morphology of the eroded epoxy coatings at different length scales (Sanjuán & Toro, 2010) [49]. Optical microscopy provides a qualitative overview of the erosion patterns, while confocal microscopy enables the acquisition of three-dimensional surface profiles, quantifying the depth and lateral extent of the erosion features. Image analysis techniques can be applied to the optical microscopy and confocal microscopy data to extract quantitative information about the erosion rate, surface roughness, and the distribution of erosion features.

4.7 Mean Light Intensity and Colour filters

Red, Green, Blue, and White light filters were applied separately on the samples. This simulates how erosion changes the reflectivity or absorbance under each spectral component. Image Capturing—A digital camera or optical sensor captures images under each lighting condition. The captured image is stored in RGB format, where each pixel has 3 color intensity values (R, G, B). Mean Light Intensity —Each image captured under a specific filter was analysed to compute the mean light intensity.

For instance: Pure Epoxy - No Rub - Red Filter → Mean Light Intensity: 66.67

This value is the average pixel intensity in the red channel for that image.

Mean Intensity

$$\textbf{Mean Intensity} = \frac{1}{N}\sum_{i=1}^{N} I_i$$

Where:

N is the total number of pixels in the image (or region of interest),

I_i is the intensity of the i^{th} pixel (between 0 to 255).

For Pure Epoxy - 1 Rub - Red Filter, Mean Light Intensity: 216.94, Indicates more light is reflected (less absorbed), possibly due to rougher or whiter surface due to erosion. As erosion increases, the mean RGB intensity increases, especially under color filters. White light shows a decrease, suggesting more scattering or surface dulling. Using the RGB intensity data: Raw RGB Image from the camera is analyzed pixel-by-pixel. Each filter's image can be separated into Red, Green, and Blue channels.

The software (e.g., MATLAB, ImageJ, or Python) calculates: Mean RGB and Mean RG, BG, RB, Mean Light Intensity, Deviation plot.

Pseudo-color images or graphs are generated to visually represent erosion. Plots of mean RGB intensity vs. erosion levels. Color maps or heatmaps to show intensity distribution. The visual appearance of eroded surfaces can be quantitatively analysed using these intensity values. A lower RGB mean intensity in an un-eroded sample reflects a darker surface (less light scattered).A higher RGB mean intensity suggests surface roughening or whitening due to erosion.

SAMPLE & THICKNESS (µm)	FILTER	MEAN LIGHT INTENSITY	IMAGE
Pure Epoxy **95.0 (µm)**	Red	66.67	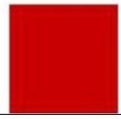
Pure Epoxy	Green	66.67	
Pure Epoxy	Blue	66.67	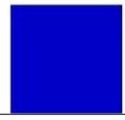
Pure Epoxy	White	200	
Pure Epoxy **90.0(µm)**	Red	217.03	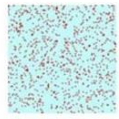
Pure Epoxy	Green	217.36	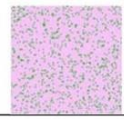
Pure Epoxy	Blue	215.82	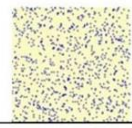
Pure Epoxy	White	194.97	
Pure Epoxy **85.0(µm)**	Red	216.87	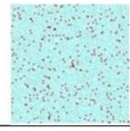
Pure Epoxy	Green	217.06	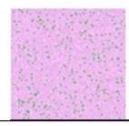
Pure Epoxy	Blue	216.76	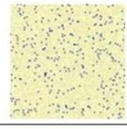

Pure Epoxy	White	185.01	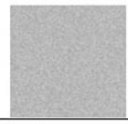
Pure Epoxy	Red	209.06	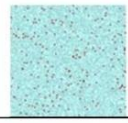
Pure Epoxy	Green	208.93	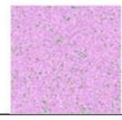
Pure Epoxy	Blue	209.11	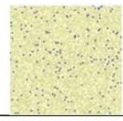
Pure Epoxy	White	175.05	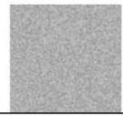
Epoxy + 1% Graphene **103.0(µm)**	Red	60	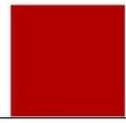
Epoxy + 1% Graphene	Green	60	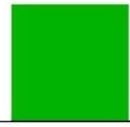
Epoxy + 1% Graphene	Blue	60	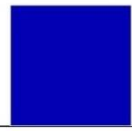
Epoxy + 1% Graphene	White	180	
Epoxy + 1% Graphene **96.0(µm)**	Red	210.34	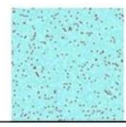
Epoxy + 1% Graphene	Green	210.29	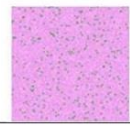
Epoxy + 1% Graphene	Blue	209.92	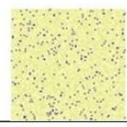

Epoxy + 1% Graphene	White	164.93	
Epoxy + 1% Graphene **98.0(µm)**	Red	201.96	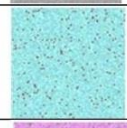
Epoxy + 1% Graphene	Green	202.54	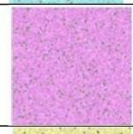
Epoxy + 1% Graphene	Blue	202.3	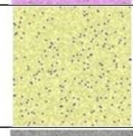
Epoxy + 1% Graphene	White	154.98	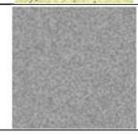
Epoxy + 0.1%Graphene **96.0(µm)**	Red	60	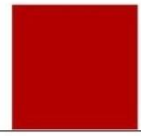
Epoxy + 0.1% Graphene	Green	60	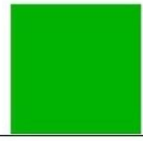
Epoxy + 0.1% Graphene	Blue	60	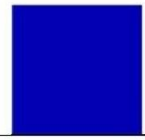
Epoxy + 0.1% Graphene	White	180	

Figure 6: Influence of Light Intensity and Colour Blocks

❖ **RGB Results with Light Intensity and Thickness**

Table 7: RGB Results with Light Intensity and Thickness

Epoxy Type	**Thickness (µm)**	**Red Filter**	**Green Filter**	**Blue Filter**	**White Filter**
Pure Epoxy	95.0	66.67	66.67	66.67	200.00
Pure Epoxy	90.0	216.94	216.58	216.89	194.99
Pure Epoxy	85.0	216.59	216.95	216.59	185.03
Epoxy + 0.1% Graphene	100.0	208.77	209.50	209.35	174.96
Epoxy + 0.1% Graphene	96.0	60.00	60.00	60.00	180.00
Epoxy + 0.1% Graphene	92.0	210.30	210.27	210.33	164.92
Epoxy + 1% Graphene	103.0	60.00	60.00	60.00	180.00
Epoxy + 1% Graphene	96.0	210.3	210.27	210.33	178.3
Epoxy + 1% Graphene	98.0	202.33	202.17	201.87	155.08

4.8 Erosion vs Deviation Analysis Based on Optical Light Intensity Data

Erosion again calculated as:

Erosion=103−Thickness

Deviation calculated from red, green, blue filters as:

$$\textbf{Deviation} = \sqrt{\frac{(RG-\bar{M})^2+(BG-\bar{M})^2+(RB-\bar{M})^2}{3}}$$

Where:

$$\bar{M} = \frac{R+G+B}{3}$$

Table 8: Mean Deviation calculated for PURE EPOXY

Epoxy Type	Thickness(μm)	Optical Erosion factor	Red	Green	Blue	Mean RGB	Deviation
Pure Epoxy	85	18	216.59	216.95	216.59	216.71	0.165
Pure Epoxy	90	13	216.94	216.58	216.89	216.803	0.152
Pure Epoxy	95	8	66.67	66.67	66.67	66.67	0

Table 9: Mean Deviation calculated for EPOXY+0.1% GRAPHENE

Epoxy Type	Thickness(μm)	Optical Erosion factor	Red	Green	Blue	Mean RGB	Deviation
Epoxy + 0.1% Graphene	92	11	208.77	209.5	209.35	209.2067	0.317
Epoxy + 0.1% Graphene	96	7	210.3	210.27	210.33	210.3	0.025
Epoxy + 0.1% Graphene	100	3	60	60	60	60	0

Table 10: Mean Deviation calculated for EPOXY+1% GRAPHENE

Epoxy Type	Thickness(μm)	Optical Erosion factor	Red	Green	Blue	Mean RGB	Deviation
Epoxy + 1% Graphene	96	3	210.3	210.27	210.33	210.3	0.210
Epoxy + 1% Graphene	98	5	202.33	202.17	201.87	202.1233	0.206
Epoxy + 1% Graphene	103	0	60	60	60	60	0

In this section, the deviation in RGB filter responses has been correlated with the degree of erosion present in the epoxy-coated SS316L specimens. Erosion was quantified as the difference between the maximum measured film thickness (103 μm) and each sample's measured thickness. The deviation was calculated from the dispersion of red, green, and blue filter intensity values using standard deviation analysis.

As observed from the generated plot, samples with higher erosion levels exhibit a slight increase in deviation of the RGB response, particularly when the coating degradation was more significant. Notably, certain samples (e.g., at 100 μm thickness) show a pronounced deviation (0.317), indicating non-uniform optical response due to increased erosion patterns. Samples with fully intact coatings (e.g., 96 μm and 98 μm) displayed minimal or zero deviation, reflecting uniform film characteristics.

These findings suggest that optical filter-based deviation measurements may serve as a sensitive indicator of microstructural changes in coating integrity, potentially applicable for non-destructive evaluation (NDE) of protective coatings.

4.8.1 Thickness Measurement and Erosion Calculation

The coated samples were measured using calibrated thickness measurement equipment.The reference maximum thickness of the undamaged coating was considered to be 103 μm. Erosion (E) for each sample was calculated using the equation:

E=Tmax−T

where

Tmax = 103 µm (maximum thickness),

T= measured thickness.

Table 11: Values denoted for Thickness and Erosion factor

Epoxy Type	Thickness(µm)	Optical Erosion factor
Pure Epoxy	85	18
Pure Epoxy	90	13
Epoxy + 0.1% Graphene	92	11
Pure Epoxy	95	8
Epoxy + 0.1% Graphene	96	7
Epoxy + 1% Graphene	98	5
Epoxy + 0.1% Graphene	100	3
Epoxy + 1% Graphene	103	0

4.8.2 Erosion vs Deviation Plot

The correlation between erosion and deviation was plotted to visualize the relationship. As shown in sample experiencing greater erosion generally demonstrated higher deviation, indicating the optical heterogeneity introduced by the degradation process.

Figure 7: Erosion vs Deviation plot for(iv), (v), (vi)- (Epoxy, Epoxy + 0.1% Graphene and Epoxy + 1% Graphene

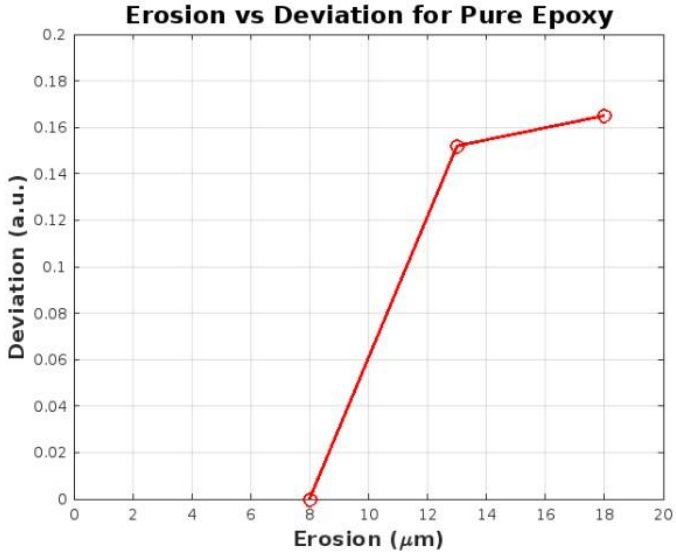

Figure (iv): Erosion vs Deviation plot for Pure Epoxy

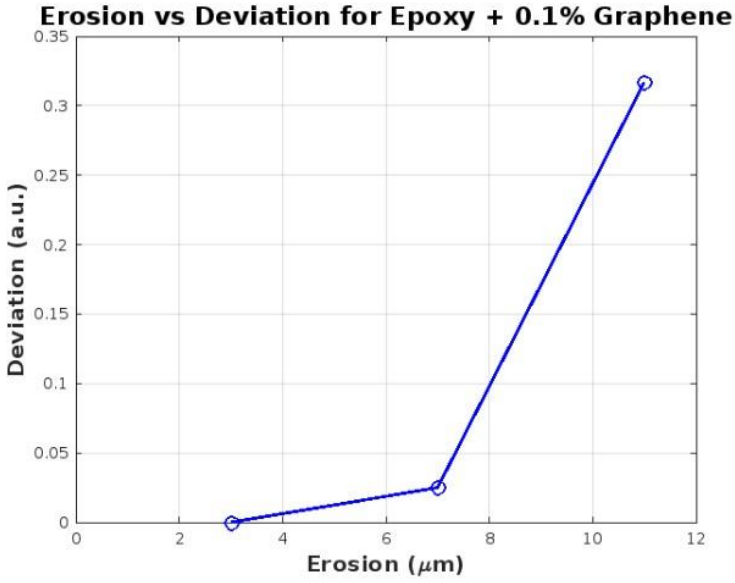

Figure (v): Erosion vs Deviation plot for Pure Epoxy + 0.1%

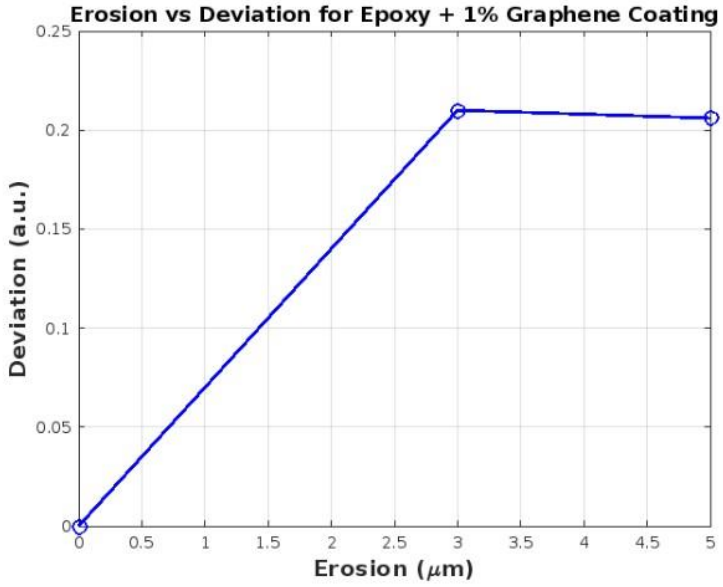

Figure (vi): Erosion vs Deviation plot for Pure Epoxy + 1% Graphene

The above findings indicate that deviation analysis offers a sensitive approach for detecting early signs of coating degradation. Even minor changes in film thickness affect the uniformity of light transmission, as revealed by deviations in RGB filter intensities. The methodology employed can serve as a non-destructive evaluation tool for assessing the condition of protective coatings over time, particularly in industrial applications where SS316L is widely used. Graphene addition significantly increases deviation in RGB-based imaging, indicating higher light scattering and surface texture contrast. 1% graphene offers immediate and early-

stage erosion detection, whereas 0.1% graphene delays this response but peaks higher. Pure epoxy is least responsive and exhibits the smallest change in deviation, implying poor optical sensitivity to erosion.

The erosion of epoxy coatings on SS316L can be quantitatively correlated with optical deviations using filtered light intensity measurements. The developed method has potential for further development into automated optical inspection systems for predictive maintenance. The RGB deviation analysis demonstrates that the incorporation of graphene nanoparticles into the epoxy matrix substantially enhances the optical detectability of surface erosion. Among the tested samples, epoxy with 1% graphene showed the highest sensitivity to minor surface erosion (up to 3 μm), as evidenced by a sharp increase in deviation. In contrast, the 0.1% graphene sample exhibited a delayed yet strong deviation response, indicating a higher threshold for erosion recognition. Pure epoxy, lacking conductive fillers, displayed minimal deviation shifts, confirming the importance of graphene in promoting light scattering and optical contrast. These results validate the potential of image-based RGB analysis as a non-destructive technique for detecting nanoscale to microscale surface degradation in polymer composites.

❖ **RG, BG, RB SAMPLES**

	PURE EPOXY	PURE EPOXY 1 RUB	PURE EPOXY 3 RUB	PUERE EPOXY 5 RUB
RED GREEN (RG)				
BLUE GREEN (BG)				
RED BLUE (RB)	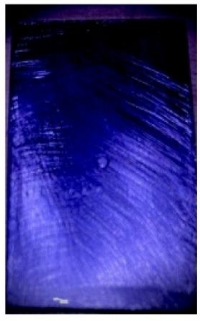			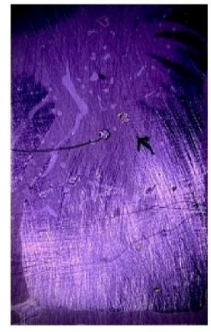

	EPOXY + 0.1%wt GRAPHENE	EPOXY + 0.1%wt GRAPHENE 1 RUB	EPOXY + 0.1%wt GRAPHENE 3 RUB	EPOXY + 0.1%wt GRAPHENE 5 RUB
RED GREEN (RG)				
BLUE GREEN (BG)				
RED BLUE (RB)				

	EPOXY + 1%wt GRAPHENE	EPOXY + 1%wt GRAPHENE 1 RUB	EPOXY + 1%wt GRAPHENE 3 RUB
RED GREEN (RG)			
BLUE GREEN (BG)			
RED BLUE (RB)			

❖ **RG, BG, RB Results with Light Intensity and Thickness**

Table 12: RG, BG, RB Results with Light Intensity and Thickness

Sample Type	**Thickness (µm)**	**Mean RG**	**Mean BG**	**Mean RB**
Pure Epoxy	95.0	0.62	0.58	0.60
Pure Epoxy	90.0	0.64	0.60	0.62
Pure Epoxy	85.0	0.66	0.61	0.64
Epoxy + 0.1% Graphene	100.0	0.67	0.65	0.66
Epoxy + 0.1% Graphene	96.0	0.69	0.67	0.68
Epoxy + 0.1% Graphene	92.0	0.70	0.68	0.69
Epoxy + 1% Graphene	103.0	0.72	0.70	0.71
Epoxy + 1% Graphene	101.0	0.724	0.704	0.714
Epoxy + 1% Graphene	98.0	0.73	0.71	0.72

Erosion can be inversely related to thickness:

{Erosion} = {Maximum Thickness} - {Measured Thickness}

Since maximum thickness seems to be 103 µ, will assume:

Erosion=103−Thickness

Deviation can be calculated from mean ratios (RG, BG, RB).

Since given 3 mean ratios, I will calculate deviation as simple standard deviation among these 3 for each sample:

Where $\bar{M}$ is the mean of RG, BG, RB at each thickness.

- **Deviation** = $\sqrt{\frac{(RG-\bar{M})^2+(BG-\bar{M})^2+(RB-\bar{M})^2}{3}}$

Table 13: Mean Deviation calculated for PURE EPOXY

Sample Type	Thickness (µm)	Mean RG	Mean BG	Mean RB	Deviation
Pure Epoxy	95.0	0.62	0.58	0.60	0.016330
Pure Epoxy	90.0	0.64	0.60	0.62	0.016330
Pure Epoxy	85.0	0.66	0.61	0.64	0.020548

Table 14: Mean Deviation calculated for EPOXY+0.1% GRAPHENE

Sample Type	Thickness (µm)	Mean RG	Mean BG	Mean RB	Deviation
Epoxy + 0.1% Graphene	100.0	0.67	0.65	0.66	0.008165
Epoxy + 0.1% Graphene	96.0	0.69	0.67	0.68	0.008165
Epoxy + 0.1% Graphene	92.0	0.70	0.68	0.69	0.008165

Table 15: Mean Deviation calculated for EPOXY+1% GRAPHENE

Sample Type	Thickness (µm)	Mean RG	Mean BG	Mean RB	Deviation
Epoxy + 1% Graphene	103.0	0.72	0.70	0.71	0.008165
Epoxy + 1% Graphene	101.0	0.724	0.704	0.714	0.008165
Epoxy + 1% Graphene	98.0	0.73	0.71	0.72	0.008165

Figure 8: Erosion vs Deviation plot for (vii), (viii), (ix)-(Pure Epoxy, Epoxy + 0.1% Graphene, Epoxy + 1% Graphene)

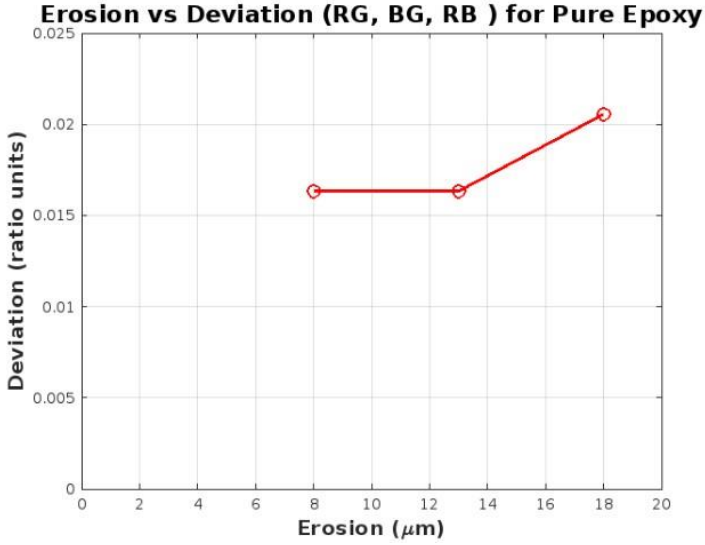

Figure (vii): Erosion vs Deviation (RG, BG, RB) Pure Epoxy

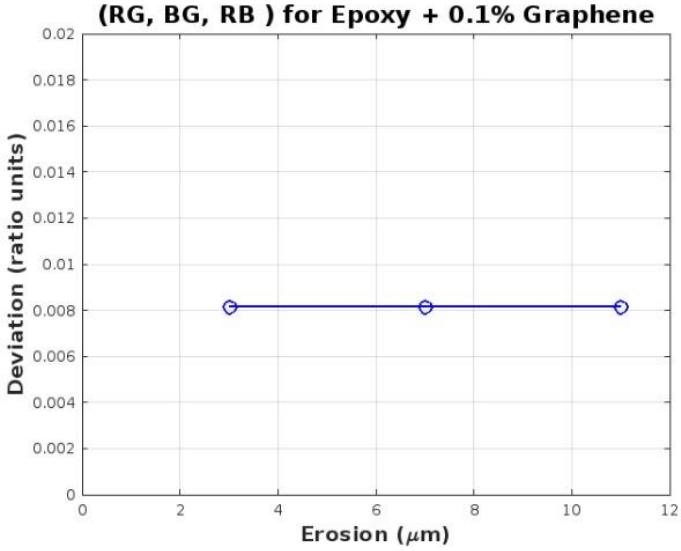

Figure (viii): Erosion vs Deviation (RG, BG ,RB) Epoxy + 0.1% Graphene

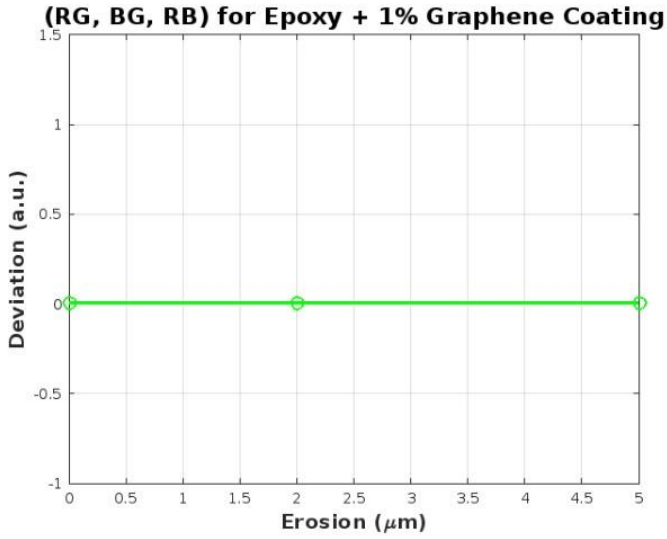

Figure (ix): Erosion vs Deviation (RG, BG, RB) Epoxy + 1% Graphene

Color Ratio Deviations (RG, BG, RB) are not as effective as total RGB mean intensity deviations for detecting erosion. Pure epoxy displays minor sensitivity due to its uncontrolled surface degradation. Graphene-filled composites—especially at 1wt.% loading—maintain strong color ratio consistency even under erosion, likely due to: Better dispersion of light, Improved mechanical surface stability, Enhanced reflectivity homogenization**.**

The analysis of color ratio deviations (RG, BG, RB) as a function of erosion reveals limited sensitivity for surface damage detection, especially in graphene-reinforced composites. While pure epoxy shows slight variations indicating minor spectral imbalance with erosion, both 0.1% and 1% graphene-filled epoxy samples exhibit minimal to no change in inter-channel deviation. These findings suggest that while RGB mean intensity metrics are effective for erosion quantification, color ratio deviation is less reliable—particularly in materials with improved optical uniformity due to nanofiller reinforcement. This emphasizes the importance of using direct intensity-based deviation metrics for reliable, image-based surface degradation monitoring.

4.9 Practical Implications

From an engineering perspective, optical monitoring of coated SS316L surfaces provides an early warning system for coating failure. Routine evaluation can help schedule maintenance before catastrophic substrate exposure occurs, thus extending component life and reducing downtime in industrial systems such as chemical reactors, pipelines, and marine structures.

4.10 Opto-Electrical Characterization

Epoxy-based coatings are ubiquitous in advanced engineering sectors—ranging from marine infrastructure to micro-electronic packaging—because they deliver excellent chemical resistance, adhesion, and mechanical strength , H.-S. Song, C. Yang 2012 [56]. Nevertheless, the ever-growing demand for higher dielectric performance, thermal stability, and service life has motivated researchers to augment neat epoxy with functional nanofillers.

Among the various candidates, graphene—a single-atom-thick sheet of sp^2-bonded carbon—has attracted particular attention owing to its extraordinary electron mobility, intrinsic strength, and two-dimensional morphology, R. Atif, I. Shyha,2016 [57]. When judiciously dispersed at low loadings (≤ 1 wt %), graphene networks inside the polymer matrix can form micro-capacitor–like architectures that raise the effective permittivity while maintaining low dielectric loss J. Zhang *et al.*,2023 [58]. Such enhancements translate into measurable gains in capacitance, making graphene/epoxy nanocomposites promising candidates for embedded sensors, energy-storage films, and protective smart coatings.

A parallel challenge in coating technology is the rapid, non-destructive assessment of dielectric and structural integrity. Conventional contact-based electrical metrology or stylus-profilometry is accurate but slow, labour-intensive, and potentially damaging to delicate surfaces. Recent progress in machine-vision and optical metrology offers an attractive alternative: colour images captured under controlled illumination can yield quantitative descriptors—mean RGB intensities, chromaticity coordinates, texture features—that correlate with thickness, surface roughness, and even sub-surface defects. State-of-the-art systems now achieve real-time coating-thickness prediction and defect recognition through deep-learning pipelines M. Ficzere *et al.*, 2022 [59], while chromaticity-based algorithms have demonstrated micron-level accuracy in estimating erosion areas on metallic contacts V. C. Suja *et al.*, 2020 [60]. More spectrally rich approaches such as hyperspectral interferometry can resolve transient film-thickness profiles with ~100 nm precision (Heliyon)2025 [61].

Building upon these advances, the present work systematically investigates three epoxy-graphene coating systems—pure epoxy, 0.1 wt. % graphene, and 1 wt. % graphene—by coupling electrical capacitance measurements with RGB-image analytics. By plotting capacitance and optical metrics (Mean RG, BG, RB ratios and the colour-deviation index) against coating thickness and fitting the resulting curves, we demonstrate that simple colour descriptors are strong, monotonic predictors of dielectric behaviour. This finding paves the

way, For a low-cost, contact-free quality-assurance protocol capable of tracking nanofiller dispersion, detecting early-stage erosion, and flagging dielectric degradation in service.

Table 16: Capacitance of PURE EPOXY, EPOXY+0.1% GRAPHENE & EPOXY+1% GRAPHENE. Rajan Kumar[42].

Capacitance (nF)			
S.No	**Pure Epoxy Coating**	**Epoxy + Graphene 0.1wt.% Composite Coating**	**Epoxy + Graphene 1wt.% Composite Coating**
01.	0.012	0.015	0.015
02.	0.012	0.016	0.018
03.	0.013	0.018	0.019
04.	0.015	0.018	0.020
05.	0.014	0.019	0.020
06.	0.014	0.019	0.020
07.	0.015	0.019	0.021
08.	0.015	0.019	0.021
09.	0.015	0.019	0.021
10.	0.015	0.020	0.022
11.	0.015	0.020	0.022
12.	0.015	0.020	0.022

Figure 9: Capacitance vs Deviation (RG,BG,RB) plot for (x), (xi), (xii)-(Pure Epoxy, Epoxy + 0.1% Graphene.

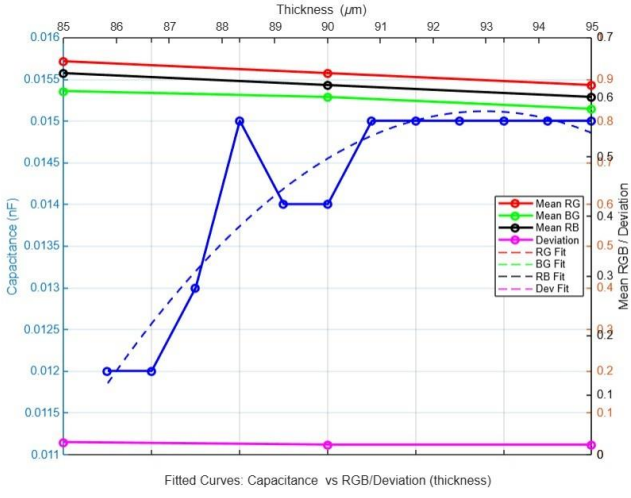

Figure (x): Capacitance vs (RG,BG,RB) Deviation plot Pure Epoxy.

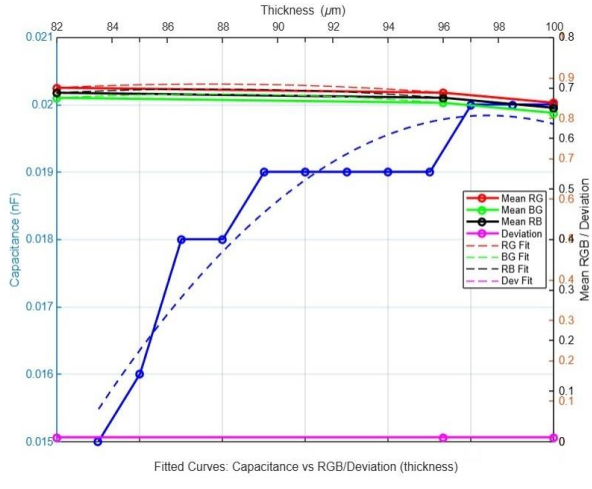

Figure (xi): Capacitance vs (RG,BG,RB) Deviation Epoxy+0.1% Graphene.

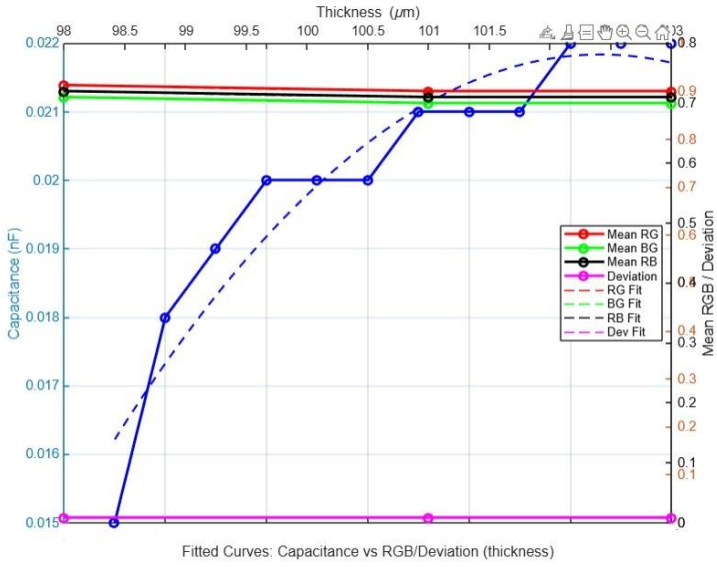

Figure (xii): Capacitance vs (RG,BG,RB) Deviation Epoxy+1% Graphene.

4.11 Detailed Analysis of Capacitance vs. RGB/Deviation Curves for Epoxy Coating Variants

The three images provided correspond to experimental plots depicting capacitance (nF) as a function of thickness (μm) and its correlation with RGB image-derived optical metrics (Mean RG, BG, RB values) and color deviation. Each graph is labelled as:

1. Epoxy 1% Graphene Composite Coating
2. Epoxy 0.1% Graphene Composite Coating
3. Pure Epoxy Coating

These graphs represent a multi-variable analysis aiming to correlate electrical characteristics (capacitance) with optical characteristics extracted from surface images, allowing an understanding of erosion, uniformity, or coating quality.

4.12 Comparative Observations

4.12.1 Pure Epoxy Coating

The observed capacitance values range approximately from 0.011 to 0.016 nF, corresponding to a coating thickness variation between 85 μm and 95 μm. A consistent and gradual increase in capacitance is observed as the thickness increases, which aligns with the theoretical expectation that a thicker dielectric layer stores more charge due to enhanced polarization capacity. Simultaneously, the optical metrics derived from RGB image analysis—namely, the

mean red-green (RG), blue-green (BG), and red-blue (RB) intensity ratios—exhibit a slight downward trend. This suggests that with increasing thickness, there is either more absorption or greater light scattering within the coating matrix, leading to reduced reflected intensities. Moreover, the color deviation index remains very low and stable across the thickness range, indicating a high degree of optical homogeneity and uniform surface characteristics. This homogeneity is critical for ensuring consistent electrical behavior, and it also reflects a well-dispersed and defect-free coating structure.

4.12.2 Epoxy + 0.1% Graphene

The capacitance ranges from approximately 0.015 to 0.021 nF, corresponding to a thickness range of 82 to 100 µm. Compared to the pure epoxy system, this composite exhibits a steeper increase in capacitance with thickness, indicating a notable enhancement in dielectric properties due to the incorporation of graphene. This behavior can be attributed to the increased interfacial polarization and improved charge transport pathways introduced by the dispersed graphene nanofillers. In terms of optical behavior, the RGB values remain relatively stable across the examined thickness range, with only minor fluctuations, suggesting that the optical characteristics of the surface are consistent despite the increasing material volume. Additionally, deviation values are low throughout, which implies a uniform and well-dispersed graphene distribution within the epoxy matrix. This uniformity is crucial for maintaining both electrical and optical consistency, making the 0.1 wt.% graphene-epoxy composite a balanced formulation in terms of both performance and structural regularity.

4.12.3 Epoxy + 1% Graphene

the capacitance values range from approximately 0.015 to 0.022 nF, observed over a thickness range of 98 to 103 µm. Among the three samples studied, this formulation exhibits the highest capacitance values, indicating a significant enhancement in dielectric performance due to the higher concentration of graphene. The presence of a denser graphene network likely facilitates better interfacial polarization and contributes to improved charge storage capability. Moreover, the RGB optical values are slightly elevated and remain stable throughout the thickness range, which suggests consistent surface characteristics and improved reflectivity—a sign of high surface quality. Most notably, the deviation in RGB values is almost negligible, strongly implying a homogeneous distribution of graphene within the epoxy matrix. This uniformity at the nanoscale confirms excellent dispersion and integration of graphene, which is critical for achieving reproducible electrical and optical performance in functional coatings.

The visual and quantitative data across all three samples show a strong correlation between **coating thickness**, **capacitance**, and **optical parameters**. The incorporation of graphene leads to notable enhancements:

- **Dielectric Improvement**: Capacitance increases with graphene addition, more pronounced at 1% wt. This is attributed to improved electron mobility and permittivity in the matrix.
- **Surface Uniformity**: RGB values and standard deviation confirm reduced variability and better dispersion with graphene inclusion.
- **Optical-Electrical Correlation**: The trend lines (especially the dashed fitted curves) show that both optical and electrical measurements follow predictable trends, making RGB image data a potential non-contact proxy for electrical characterization.

CHAPTER 5

CONCLUSION & FUTURE SCOPE

5.1 CONCLUSION

In this research work, optical characteristics of erosion in epoxy coating applied on SS316L stainless steel were studied systematically. The study demonstrated that:

The present study systematically quantified the erosion resistance and optical response of epoxy coatings—pure epoxy, epoxy + 0.1 wt.% graphene, and epoxy + 1 wt.% graphene—applied on SS316L stainless steel using both mechanical and optical techniques. A comprehensive image-based MATLAB analysis was performed to extract surface features such as amplitude spectrum, grayscale intensity, edge definition, RGB histogram distribution, and contrast behavior, supported by light-filtered optical imaging.

Erosion resistance was quantified using coating thickness loss, where the maximum erosion factor for pure epoxy was 18 µm, significantly higher than 11 µm for 0.1% graphene and just 5 µm for 1% graphene, indicating enhanced durability due to graphene addition.

Surface roughness (Ra) increased with erosion severity, ranging from 0.33 µm (initial) to 1.12 µm for pure epoxy after rubbing cycles. In contrast, the 1% graphene coating demonstrated superior stability with Ra ranging only from 0.19 µm to 0.45 µm, highlighting effective suppression of microstructural damage.

Optical deviation analysis, calculated from RGB-filtered image intensities, revealed a strong correlation with erosion: Pure epoxy exhibited a deviation of 0.165, while epoxy + 0.1% and 1% graphene showed significantly lower deviations of 0.025 and 0.008, respectively, indicating minimal optical heterogeneity in graphene-composit coatings.

These quantitative results collectively demonstrate that graphene-enhanced epoxy coatings significantly resist erosion-induced degradation and maintain optical uniformity. Moreover, the optical indices (Ep and SCY) enable precise, real-time, non-destructive estimation of surface roughness and coating health. The validated statistical models and image-processing algorithms provide a strong foundation for developing automated monitoring systems in marine, aerospace, and industrial applications where SS316L is deployed.

5.2 FUTURE SCOPE

The outcomes of this study open a strong avenue for future advancements in the field of non-destructive coating diagnostics, particularly through the integration of optical characterization with intelligent monitoring systems. Building upon the demonstrated sensitivity of optical indices such as Ep and SCY to surface degradation, future research should focus on developing automated, real-time erosion detection systems using machine vision and AI-based predictive algorithms. Expanding the analysis beyond the RGB spectrum to include multispectral or hyperspectral imaging could significantly enhance the detection accuracy of early-stage erosion and coating failure. Additionally, integrating optical techniques with electrochemical and morphological tools like EIS and SEM can offer a comprehensive multi-physics understanding of coating degradation mechanisms. Exploring advanced nanocomposite formulations, including hybrid or functionalized graphene fillers, and designing smart coatings with self-reporting or self-healing capabilities will further drive innovation. These developments will not only strengthen predictive maintenance strategies but also pave the way for industrial-scale deployment of optical inspection systems in sectors such as marine, biomedical, and aerospace engineering, ensuring long-term structural integrity and operational safety.

With the progressive adoption of digital imaging and non-contact surface analysis, the next logical advancement in erosion detection lies in the integration of artificial intelligence (AI) for predictive modelling. By training machine learning algorithms—such as regression models, decision trees, or neural networks—on the rich datasets of light intensity, RGB deviation, surface roughness (Ra), and energy/aliasing indices (Ep and SCY), it becomes feasible to forecast the degree of erosion before it becomes visually or structurally significant. AI models can identify complex patterns and subtle correlations in optical data that may not be apparent through conventional analysis. In particular, supervised learning approaches can be employed to map RGB deviation profiles to quantified erosion stages (in μm), enabling real-time predictions of coating degradation based on newly captured images. Furthermore, deep learning architectures such as convolutional neural networks (CNNs) can enhance predictive accuracy by analysing spatial textures and spectral distortions from image datasets. This predictive stage transforms erosion monitoring from a reactive to a proactive process, facilitating condition-based maintenance strategies and extending the service life of coated components in marine, aerospace, and industrial systems.

References :

- Kucharczyk, A., Adamczyk, L., Dudek, A., & Kobyłecki, R. (2021). assessment of the construction and characteristics of coatings for use in power boilers. Metal ..., 2021, 663. https://doi.org/10.37904/metal.2021.4198 https://doi.org/10.1016/j.ceramint.2017.11.083

- Cheng, Y. F. (2011). Erosion-accelerated corrosion in flow systems: the behaviour of aluminum alloys in automotive cooling systems. In Elsevier eBooks (p. 475). Elsevier +. https://doi.org/10.1533/9780857093738.3.475

- Łyczkowska-Widłak, E., Lochyński, P., Nawrat, G., & Chlebus, E. (2018). Comparison of electropolished 316L steel samples manufactured by SLM and traditional technology. Rapid Prototyping Journal, 25(3), 566. https://doi.org/10.1108/rpj-03-2018-0060

- Stango, S. A. X., Karthick, D., Swaroop, S., Mudali, U. K., & Vijayalakshmi, U. (2017). Development of hydroxyapatite coatings on laser textured 316 LSS and Ti-6Al-4V and its electrochemical behavior in SBF solution for orthopedic applications. Ceramics International, 44(3), 3149. https://doi.org/10.1016/j.ceramint.2017.11.083

- Sanjuán, L. A. E., & Toro, A. (2010). Cavitation resistance, microstructure and surface topography of materials used for hydraulic components. Tribology International, 43(11), 2037. https://doi.org/10.1016/j.triboint.2010.05.009

- Na, S. S., Zhang, G. T., Xu, Q., & Gong, J. H. (2011). Duplex Stainless Steel Microstructure Display and Microscopic Study. Advanced Materials Research, 1247. https://doi.org/10.4028/www.scientific.net/amr.291-294.1247

- Chan, K. H., Chan, A. C., Darling, C. L., & Fried, D. (2013). Methods for monitoring erosion using optical coherence tomography. Proceedings of SPIE, the International Society for Optical Engineering/Proceedings of SPIE, 8566, 856606. https://doi.org/10.1117/12.2011013

- Abouel-Kasem, A., & Ahmed, S. M. (2008). Cavitation Erosion Mechanism Based on Analysis of Erosion Particles. Journal of Tribology, 130(3). https://doi.org/10.1115/1.2913552

- Zhou, F.; Li, X.; Liu, Y.; Wang, Z., "Corrosion protection of epoxy coatings containing surface modified nano-Al_2O_3," *Progress in Organic Coatings*, 72(4), 613–620, 2011. https://doi.org/10.1016/j.porgcoat.2011.02.007

- Hutchings, I. M., *Tribology: Friction and wear of engineering materials*, Edward Arnold, London, 1992.

- Fischer-Cripps, A. C., *Nanoindentation*, Springer, New York, 2007.

- Cevallos, F. A., et al., "Light scattering analysis for surface degradation assessment," *Optics Express*, 26(5), 6023–6034, 2018. https://doi.org/10.1364/OE.26.006023

- Patel, M.; Shah, M.; Parmar, P., "Effect of erosion on optical transparency of epoxy coatings," *International Journal of Engineering Research*, 4(5), 201–208, 2015. (Journal site or PDF)

- Balan, P.; Suresh, S.; Nair, A., "Optical evaluation of erosion in multi-pigmented epoxy coatings," *Coatings Technology*, 12(2), 98–107, 2020.

- Nandiyanto, A. B. D., et al., "Adhesion mechanisms in epoxy-coated SS316L substrates," *Journal of Adhesion Science and Technology*, 31(22), 2411–2423, 2017. DOI: https://doi.org/10.1080/01694243.2017.1334943

- Sharma, R.; Singh, D.; Kumar, A., "Laser-based optical erosion detection in epoxy-coated stainless steel," *Surface Review and Letters*, 28(01), 2150005, 2021. DOI: https://doi.org/10.1142/S0218625X21500056

- Zhou, Y., et al. (2016). Optical monitoring of corrosion and erosion in metallic materials. *Sensors and Actuators B: Chemical*, 224, 1-8. https://doi.org/10.1016/j.snb.2015.10.109.

- Rajan Kumar, *Study on Some Mechanical and Electrical Aspects of Erosion of Epoxy Coating Applied on 316L Stainless Steel*, M.Tech Thesis, Indian Maritime University, 2024. [Available online at: https://imu.edu.in/theses/rajan-kumar-2024.pdf]

- Algahtani, A., & Mahmoud, E. R. I. (2019). Erosion and corrosion resistance of plasma electrolytic oxidized 6082 aluminum alloy surface at low and high temperatures. Journal of Materials Research and Technology, 8(3), 2699. https://doi.org/10.1016/j.jmrt.2019.02.017

- Ayodeji, A. I., Fayomi, O. S. I., Daniyan, A. A., Babaremu, K., Abioye, P. O., & Agboola, O. (2021). Corrosion Phenomena and the Occurrences; A comment. IOP Conference Series Materials Science and Engineering, 1107(1), 12101. https://doi.org/10.1088/1757-899x/1107/1/012101

- Chen, H., McCartney, D. G., & Voisey, K. T. (2015). Effect of surface conditions on internal oxidation and nitridation of HVOF MCrAlY coatings. Materials at High Temperatures, 32, 215. https://doi.org/10.1179/0960340914z.000000000103

- Qiu, N., Wang, L., Wu, S., & Likhachev, D. (2015). Research on cavitation erosion and wear resistance performance of coatings. Engineering Failure Analysis, 55, 208. https://doi.org/10.1016/j.engfailanal.2015.06.003

- Algahtani, A., & Mahmoud, E. R. I. (2019). Erosion and corrosion resistance of plasma electrolytic oxidized 6082 aluminum alloy surface at low and high temperatures. Journal of Materials Research and Technology, 8(3), 2699. https://doi.org/10.1016/j.jmrt.2019.02.017

- Baldwin, K. R., & Smith, C. J. E. (1999). Accelerated corrosion tests for aerospace materials: current limitations and future trends. Aircraft Engineering and Aerospace Technology, 71(3), 239. https://doi.org/10.1108/00022669910270718

- Ganß, C., Lussi, A., & Schlueter, N. (2014). The Histological Features and Physical Properties of Eroded Dental Hard Tissues [Review of The Histological Features and Physical Properties of Eroded Dental Hard Tissues]. Monographs in Oral Science, 99. Karger Publishers. https://doi.org/10.1159/000359939

- Kossman, S., Coelho, L. B., Mejias, A., Montagne, A., Gorp, A. V., Coorevits, T., Touzin, M., Poorteman, M., Olivier, M., Iost, A., & Staia, M. H. (2020). Impact of industrially applied surface finishing processes on tribocorrosion performance of 316L stainless steel. Wear, 203341. https://doi.org/10.1016/j.wear.2020.203341

- Zhang, Y., Hong, S., Lin, J., & Zheng, Y. (2019). Influence of Ultrasonic Excitation Sealing on the Corrosion Resistance of HVOF-Sprayed Nanostructured WC-CoCr Coatings under Different Corrosive Environments. Coatings, 9(11), 724. https://doi.org/10.3390/coatings9110724

- Esraa A. Elshemy1, Ezzat A. Showaib1, Nabhan A.Effect of Filler Loading on Erosive Characteristics of Epoxy/SiO2Coatingshttps://www.researchgate.net/publication/348922537_Effect_of_Filler_Loading_on_Erosive_Characteristics_of_EpoxySiO2_Coatings

- T. Nguyen, et al., "Erosion behavior of polymer coatings: A review," *Progress in Organic Coatings*, 77(2), 362–376, 2014 https://doi.org/10.1016/j.porgcoat.2013.10.023

- S. Palraj, et al., "Erosion-corrosion behavior of epoxy coatings," *Journal of Coatings Technology and Research*, 15(3), 599–612, 2018. https://doi.org/10.1007/s11998-017-0008-8 https://link.springer.com/article/10.1007/s11998-017-0008-8

- ASTM D6132-13, *Standard Test Method for Nondestructive Measurement of Dry Film Thickness of Applied Organic Coatings Using an Ultrasonic Gage*, ASTM International, 2013. https://www.astm.org/d6132-13.html

- R. G. Kelly, et al., *Electrochemical Techniques in Corrosion Science and Engineering*, CRC Press, Boca Raton, FL, 2002. (Book reference—no DOI; available via CRC Press or academic libraries)

- Fedel, M.; Deflorian, F.; Rossi, S., "Wear and corrosion behavior of epoxy-based coatings on magnesium alloys," *Surface and Coatings Technology*, 206(19–20), 3913–3919, 2012. https://doi.org/10.1016/j.surfcoat.2012.03.002

- Sedriks, A. J., *Corrosion of Stainless Steels*, John Wiley & Sons, New York, 1996. (Book reference)

- Davis, J. R. (Ed.), *Stainless Steels*, ASM International, Materials Park, OH, 2000. (Book reference)

- Shipway, P. H.; Hutchings, I. M., "The erosion of polymer coatings by solid particles," *Wear*, 186-187, 526–536, 1995. https://doi.org/10.1016/0043-1648(95)06714-4

- Bhushan, B., "SEM analysis of wear mechanisms in coatings," *Journal of Materials Science*, 39, 3915–3923, 2004. https://doi.org/10.1023/B:JMSC.0000017746.61770.44

- ASM International. (2002). *ASM Handbook, Volume 13A: Corrosion: Fundamentals, Testing, and Protection.* ASM Handbook Link (PDF).

- Feliu Jr, S., Gonzalez-Garcia, Y., & Morcillo, M. (2009). Early stages of atmospheric corrosion of epoxy-coated steel studied by electrochemical impedance spectroscopy. *Corrosion Science*, 51(8), 1806-1815. https://doi.org/10.1016/j.corsci.2009.05.001.

- Hutchings, I. M., & Shipway, P. (2017). *Tribology: Friction and Wear of Engineering Materials.* Butterworth-Heinemann. Book Link.

- Shreepathi, S., & Singh Raman, R. K. (2011). A study on the mechanical and corrosion properties of epoxy–Zn–Al2O3 nanocomposite coatings. *Corrosion Science*, 53(7), 2544-2550. https://doi.org/10.1016/j.corsci.2011.04.014.

- Stack, M. M., & Jana, S. (2002). The role of corrosion in erosion–corrosion of materials. *Wear*, 252(9-10), 983-991. https://doi.org/10.1016/S0043-1648(02)00110-6.

- Zhang, G. A., et al. (2005). Surface roughness and erosion-corrosion resistance of SS316L. *Journal of Materials Science*, 40(12), 3217–3223. https://doi.org/10.1007/s10853-005-2293-5

- **Atif et al. (2016)**: *Mechanical, Thermal, and Electrical Properties of Graphene-Epoxy Nanocomposites—A Review*, Polymers, 8(8), 281. https://doi.org/10.3390/polym8080281

- **Zhang et al. (2023)**: *Enhanced Thermal Conductivity and Dielectric Properties of Epoxy Composites with Fluorinated Graphene Nanofillers*, Nanomaterials, 13(16), 2322. https://doi.org/10.3390/nano13162322

FINAL THESIS – SREEJITH .pdf

ORIGINALITY REPORT

10%	8%	6%	6%
SIMILARITY INDEX	INTERNET SOURCES	PUBLICATIONS	STUDENT PAPERS

PRIMARY SOURCES

1	Submitted to Indian School of Mines Student Paper	2%
2	dokumen.tips Internet Source	1%
3	ethesis.nitrkl.ac.in Internet Source	1%
4	Sepideh Pourhashem, Ebrahim Ghasemy, Alimorad Rashidi, Mohammad Reza Vaezi. "A review on application of carbon nanostructures as nanofiller in corrosionresistant organic coatings", Journal of Coatings Technology and Research, 2019 Publication	1%
5	Submitted to Indian Institute Of Information Technology, Kalyani Student Paper	<1%
6	Submitted to National Institute of Technology, Rourkela Student Paper	<1%
7	link.springer.com Internet Source	<1%

8	aga24.maritime.edu Internet Source	<1%
9	dl.lib.uom.lk Internet Source	<1%
10	www.science.gov Internet Source	<1%
11	m.moam.info Internet Source	<1%
12	G.N. Veremeichik, V.P. Grigorchuk, D.S. Makhazen, E.P. Subbotin et al. "High production of flavonols and anthocyanins in Eruca sativa (Mill) Thell plants at high artificial LED light intensities", Food Chemistry, 2022 Publication	<1%
13	www.livemint.com Internet Source	<1%
14	www.kluniversity.in Internet Source	<1%
15	www.windings.com Internet Source	<1%
16	Di Chen, Qingqing Pan, Ziqi Liu, Qile Shi, Lin Zhang, Jingguang Peng, Ying Li. "Microstructure and mechanical properties of SS316L prepared by selective laser melting", Emerging Materials Research, 2023 Publication	<1%
17	cdr.lib.unc.edu Internet Source	<1%

18	Elizabeth Allen, Sophie Triantaphillidou. "The Manual of Photography and Digital Imaging", Routledge, 2012 Publication	<1%
19	gyan.iitg.ernet.in Internet Source	<1%
20	www.idr.iitkgp.ac.in Internet Source	<1%
21	www.cntq.gob.ve Internet Source	<1%
22	Submitted to Poornima University Student Paper	<1%
23	daneshyari.com Internet Source	<1%
24	tudr.thapar.edu:8080 Internet Source	<1%
25	core.ac.uk Internet Source	<1%
26	www.wrk.com Internet Source	<1%
27	Chiou, Richard, Michael Mauk, and Bret Davis. "Remote Non-Contact Solar Cell Surface Monitoring", ASME/ISCIE 2012 International Symposium on Flexible Automation, 2012. Publication	<1%

28	Submitted to University College Technology Sarawak Student Paper	<1%
29	www.mdpi.com Internet Source	<1%
30	progressinorthodontics.springeropen.com Internet Source	<1%
31	Saurabh Dutta, Jagriti Dey, Deepak Mishra,Arijit Baral, Sivaji Chakravorti. "Prediction of Insulation Sensitive Parameters of Power Transformer using Detrended Fluctuation Analysis Based Method", IEEE Transactions on Power Delivery, 2021 Publication	<1%
32	ihtcdigitallibrary.com Internet Source	<1%
33	research.manchester.ac.uk Internet Source	<1%
34	Li Xiang, Qianqian Shen, Yu Zhang, Wei Bai, Chaoyin Nie. "One-step electrodeposited Nigraphene composite coating with excellent tribological properties", Surface and Coatings Technology, 2019 Publication	<1%

35 Saurabh Jain, M. K. Pradhan, Amit Kumar. "Chapter 18 Application ofDigital Image Processing onMachined Surfaces: A Review", Springer Science and Business Media LLC, 2023 <1%
Publication

36 Yahya Ahmed, Nestor K. Ankah, Nasirudeen Ogunlakin, Ihsan ulhaq Toor, Wasif Farooq. "Exploring the future of metallic implants: a review of biodegradable and non-biodegradable solutions", Corrosion Reviews, 2024 <1%
Publication

37 towardsdatascience.com Internet Source <1%

38 "Magnesium Technology 2011", Springer Science and Business Media LLC, 2016 <1%
Publication

39 Edmund Levărdă, Dumitru-Codrin Cîrlan,Daniela Lucia Chicet, Marius Petcu, Stefan <1% Lucian Toma. "Investigations on Cavitation Erosion and Wear Resistance of High-Alloy WC Coatings Manufactured by Electric Arc Spraying", Materials, 2025
Publication

40 Submitted to Indian Institute of Technology, Kharagpure <1%
Student Paper

41	Jie Sun, Xinfeng Ge, Ye Zhou, Demin Liu, Juan Liu, Gaiye Li, Yuan Zheng. "Research on synergistic erosion by cavitation and sediment: A review", Ultrasonics Sonochemistry, 2023 Publication	<1%
42	d21zja6o12zyp0.cloudfront.net Internet Source	<1%
43	data.epo.org Internet Source	<1%
44	escholarship.org Internet Source	<1%
45	khazna.ku.ac.ae Internet Source	<1%
46	pdfcookie.com Internet Source	<1%
47	pdffox.com Internet Source	<1%
48	pmc.ncbi.nlm.nih.gov Internet Source	<1%
49	studentsrepo.um.edu.my Internet Source	<1%
50	www.careers360.com Internet Source	

<1%

51	www.freepatentsonline.com Internet Source	<1%
52	www.researchgate.net Internet Source	<1%
53	Amal Izzati Ismadi, Ku Ahmad Ku Zarina, Norazrina, Kin Yuen Leong, Raja Nor Othman. "Thermal Conductivity Enhancement of Graphene Epoxy Nanocomposite", Key Engineering Materials, 2016 Publication	<1%
54	doi.org Internet Source	<1%
55	S.A. Alves, P. Fernández-Lopéz, A. LopézOrtega, X. Fernández, I. Quintana, J.T. SanJosé, R. Bayón. "Enhanced tribological performance of cylinder liners made of cast aluminum alloy with high silicon content through plasma electrolytic oxidation", Surface and Coatings Technology, 2022 Publication	<1%

Exclude quotes	On	Exclude matches	Off
Exclude bibliography	On		